In this work we examined the differentiation potential of cholangiocytes in neonatal and adult mouse liver. We found that neonatal, but not adult, epithelial cell adhesion molecule $(EpCAM)^+$ cholangiocytes expressed hepatocytic transcription factors and converted into hepatocytes *in vitro* that were structurally and functionally similar to MHs. Interestingly, neonatal cholangiocytes are still immature compared with adult ones even though they have already established tubular structures *in vivo*. Our results indicate that neonatal cholangiocytes possess plasticity to convert into hepatocytes but lose this ability during maturation of bile ducts. We further demonstrated that a transcription factor implicated in epithelial maturation limited lineage plasticity of cholangiocytes.

Results

Cholangiocytes proliferate and retain the cholangiocytic phenotype on type I collagen gel

Because the number of cholangiocytes isolated from the liver is limited and not enough to examine their differentiation potential, we first established a primary culture in which cholangiocytes keep the original characteristics and efficiently proliferate. To isolate mature cholangiocytes from 6 week old (6W) mouse liver, two step collagenase perfusion was performed and the remaining tissue containing Glisson's capsules was further digested. $EpCAM^+$ cholangiocytes were enriched by magnetic activated cell sorting (MACS; supplementary material Fig. S1). They were plated on culture wells coated with type I collagen (Col I) or a thin layer of Matrigel (MG), or covered with Col I gel or MG gel (Fig. 1A). On wells coated with Col I, only a very small number of cells survived and proliferated. On MG coated or MG gel wells, 2 or 3 days after plating, cells began to proliferate slowly. On Col I gel, cells proliferated very efficiently. In all four conditions, cells survived and proliferated after replating at day 7 of primary culture. Importantly, on Col I gel, as well as MG gel, expression of EpCAM was retained on cholangiocytes but disappeared when grown in wells coated with Col I (Fig. 1B; supplementary material Fig. S2). During the culture on Col I gel, cholangiocytes maintained expression of cholangiocyte markers [osteopontin (OPN), SRY related HMG box transcription factor 9 (Sox9) and hepatocyte nuclear factor (Hnf)1β], but did not express the hepatocyte marker, Hnf4α (Fig. 1C), and kept epithelial characteristics, such as the ability to form cystic structures in 3D culture; about 1% of cells formed cysts during 10 days in culture ever after the fourth passage (Fig. 1D; supplementary material Fig. S2). We further confirmed that, like mouse cholangiocytes, human $EpCAM^+$ cholangiocytes proliferated and retained the expression of EpCAM on Col I gel (supplementary material Fig. S3). In the following experiments, we examined differentiation potential of cholangiocytes after expansion in Col I gel culture.

Hepatocytic differentiation potential of adult cholangiocytes

To examine the hepatocytic differentiation potential of cholangiocytes, $EpCAM^+$ cells derived from 6 8W mouse livers were cultured on Col I gel for 5 days and then replated onto dishes coated with gelatin. To induce hepatocytic differentiation, oncostatin M (OSM) was added to the culture medium after the cells reached confluency. On day 9 in culture,

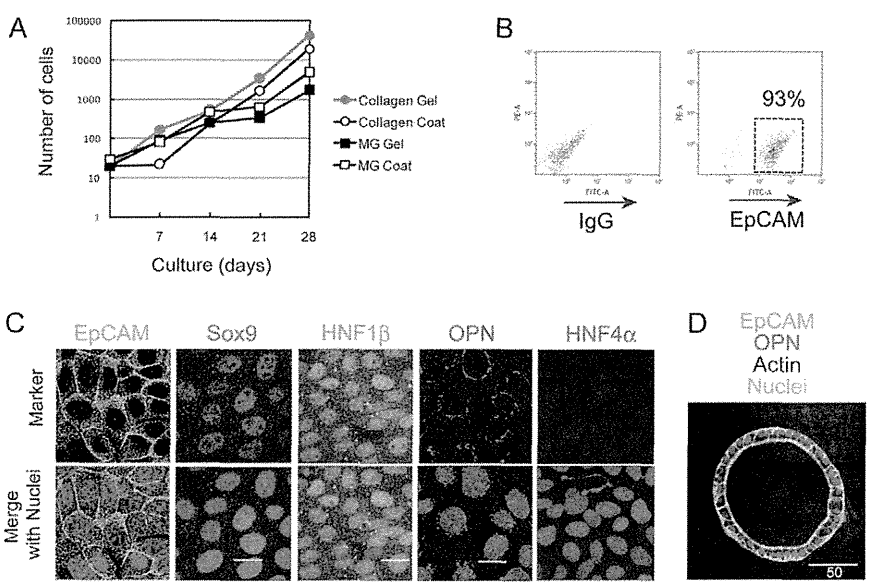

Fig. 1. *In vitro* expansion of $EpCAM^+$ cholangiocytes on Col-I gel. (A) Proliferation of $EpCAM^+$ cholangiocytes on Col-I and Matrigel®. Cholangiocytes were cultured on Col-I-coated or MG-coated wells or on Col-I gel or MG. Every 7 days, they were replated onto dishes coated with the same extracellular matrix as the primary culture. During primary culture, cholangiocytes proliferated on Col-I gel, MG gel and MG-coated dishes, though they proliferated most efficiently on Col-I gel. Beyond secondary culture, cholangiocytes proliferated in all conditions. (B) Adult cholangiocytes retained the expression of EpCAM on Col-I gel. EpCAM expression was examined by fluorescence-activated cell sorting (FACS). More than 90% of cells retained EpCAM expression on Col-I gel. (C) Adult cholangiocytes retained the expression of marker genes on Col-I gel. Cultured cholangiocytes expressed the cholangiocyte markers EpCAM, Sox9, HNF1β, and OPN. $EpCAM^+$ cells isolated from 6W mouse liver were cultured on Col-I gel for 7 days, fixed in 4% PFA, and incubated with anti-Sox9, anti-HNF1β and anti-OPN antibodies. Nuclei were counterstained with Hoechst 33258. (D) Adult cholangiocytes form cysts with the central lumen in three-dimensional culture. At day 7, cultured cholangiocytes were dissociated from Col-I gel, replated on a layer of MG, and then overlaid with 5% MG. Cysts were stained with anti-EpCAM (green), anti-OPN (red), and phalloidin (white). Nuclei were counterstained with Hoechst33258 (blue).

cells were overlaid with 5% MG (Fig. 2A). Dense cytoplasm and clear cell cell contacts were observed after sequential treatment with OSM and MG (Fig. 2B). However, as shown in Fig. 2B, the cells barely expressed hepatocyte markers including albumin, carbamoylphosphate synthetase I (CPSI), phosphoenolpyruvate carboxykinase (PEPCK), and tryptophan 2,3 dioxygenase (Tdo2). Thus, hepatocytic characteristics could not be induced in adult cholangiocytes.

Hepatocytic differentiation potential of neonatal cholangiocytes

To investigate whether cholangiocytes have the potential to differentiate into hepatocytes during the early stage of bile duct formation, we applied the same culture conditions to neonatal cholangiocytes isolated from 1W liver. Similar to adult cholangiocytes, neonatal cholangiocytes continued to express cholangiocyte markers during culture on Col I gel (supplementary material Fig. S4). As shown in Fig. 2A, neonatal cells cultured on gelatin proliferated and formed a monolayer in which the cells were in close contact with each other. After addition of OSM to the medium on day 5, the cells altered their morphology, developing round nuclei and dense cytoplasm. When the cells were overlaid with MG, cytoplasmic granularity increased. Furthermore, bile canaliculus (BC) like structures were observed between the cells. During the sequential treatment of OSM and MG, there was increased expression of the genes for albumin, metabolic enzymes including glucose 6 phosphatase (G6Pase), PEPCK, tyrosine aminotransferase (TAT), Tdo2, CPSI and cytochrome P450 proteins (Cyps) (Fig. 2B). We also examined expression of cholangiocyte markers including cytokeratin (CK) 7, CK19 and EpCAM, and found that CK7 and EpCAM were downregulated during hepatocytic differentiation (Fig. 2B and supplementary material Fig. S5). Immunocytochemical analysis showed that albumin and CPSI proteins, which were not expressed in neonatal cholangiocytes at the beginning of the culture period, were expressed in the cytoplasm after inducing hepatocytic differentiation (Fig. 2C3; Figs 4, 7, 8), whereas both proteins were not induced in adult cholangiocytes (Fig. 2C1; Figs 2, 5, 6). However, EpCAM was not downregulated in adult cholangiocytes but was in neonatal ones during culture (Fig. 2C9 12). To examine whether cells treated with MG acquired differentiated functions, ammonium chloride was added to the culture medium. The concentration of ammonium ions in the medium gradually decreased with the time in the wells of cultured neonatal cholangiocytes but not in those of adult cells

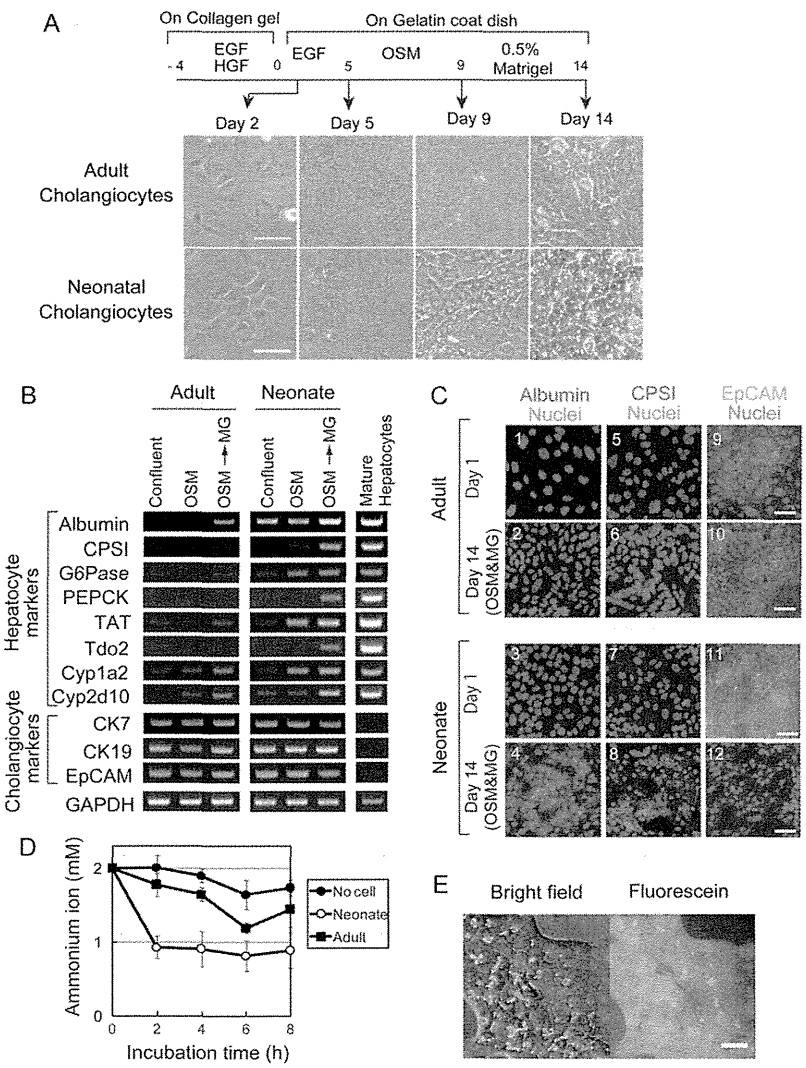

Fig. 2. Neonatal, but not adult, cholangiocytes differentiate to functional hepatocytes. (A) Morphological changes of adult and neonatal cholangiocytes during culture. Adult cholangiocytes show dense cytoplasm at day 5 in culture. Cell cell contacts were clearly visible after overlaying with MG. Neonatal cholangiocytes had round nuclei and dense cytoplasm in the presence of OSM. Cell cell contacts were more evident after overlaying with MG. After expansion on Col-I gel, adult and neonatal cholangiocytes were used to induce hepatocytic characteristics by sequentially treating them with OSM and MG. Scale bars: 50 μm. (B) Neonatal cholangiocytes were induced to express hepatocyte markers. Hepatocyte marker expression was examined by PCR. Adult cholangiocytes weakly expressed albumin but not other hepatocyte markers even in the presence of OSM and MG. In contrast, hepatocyte markers such as CPSI, G6Pase, PEPCK, TAT and Tdo2 were induced in neonatal cholangiocytes during culture. Cyp1a2 and Cyp2d10 were also expressed. Among cholangiocyte markers, CK7 and EpCAM were slightly downregulated in the presence of OSM and MG. Experiments were repeated three times, independently, and the representative data are shown. (C) Expression of hepatocyte markers at the protein level. At 1 day after plating onto gelatin-coated dishes, neonatal cholangiocytes did not express albumin and CPSI. After inducing hepatocytic differentiation, albumin (red) was expressed in many cells. Some cells expressed CPSI (red). In contrast, both proteins were not expressed in adult cholangiocytes before and after treatment of OSM and MG. Scale bars: 50 μm. (D) Hepatocytes derived from neonatal cholangiocytes eliminated ammonium ions from the medium. Ammonium chloride (2 mM) was added to neonatal cholangiocytes treated with MG. Ammonium ions in the medium were eliminated by hepatocytes derived from neonatal cholangiocytes. Average values at each time point are shown (±s.d.). (E) Hepatocytes derived from neonatal EpCAM$^+$ cells formed BC-like structures. After incubation in the presence of MG, cells were further treated with 100 μM taurocholate, and FDA was then added. Hepatocytes derived from neonatal cholangiocytes metabolized FDA and fluorescein was secreted into BC-like structures. Scale bar: 50 μm.

(Fig. 2D). Finally, to confirm whether BC like structures were generated, we added fluorescein diacetate (FDA) to the culture medium after augmenting formation of BC like structures in the presence of taurocholate (Fu et al., 2011). We found that metabolized fluorescein was excreted into BC like structures (Fig. 2E). These data indicate that cholangiocytes possessed the ability to convert into functional hepatocytes during the neonatal period.

HNF4α and C/EBPα are induced in neonatal cholangiocytes during culture

Transcription factors have been shown to determine and convert the lineages of many types of cells. At the time when hepatoblasts are committed to cholangiocytes, transcription factors related to hepatocytic differentiation, including HNF4α and CCAAT/enhancer binding protein α (C/EBPα), are suppressed, whereas those related to cholangiocytic differentiation are upregulated (Tanimizu and Miyajima, 2004; Yamasaki et al., 2006). Therefore, we tested the possibility that the expression patterns of these transcription factors differ between neonatal and mature cholangiocytes. We focused on HNF4α and C/EBPα, because both of these are crucial for the differentiation and/or maturation of hepatocytes (Parviz et al., 2003; Mackey and Darlington, 2004). Using quantitative PCR, we examined the expression of *HNF4α* and *C/EBPα* in neonatal and mature cholangiocytes during culture for hepatocytic differentiation. We also examined the expression of *FoxA1* (*HNF3α*), which has been shown to be a crucial factor conferring hepatocytic characteristics on multipotent as well as somatic cells (Sekiya et al., 2009; Sekiya and Suzuki, 2011). HNF4α and C/EBPα genes were clearly induced in neonatal but not in mature cholangiocytes, whereas *FoxA1* was expressed in both cell types (Fig. 3A). These results suggest that the efficient induction of HNF4α and C/EBPα is necessary for cholangiocytes to convert into hepatocytes. Immunofluorescence analysis further confirmed that HNF4α and C/EBPα were induced in neonatal cholangiocytes but not in adult ones after inducing hepatocytic differentiation (Fig. 3B).

Overexpression of C/EBPα and inhibition of the Notch signaling pathway slightly increase hepatocyte gene expression in mature cholangiocytes

To examine whether HNF4α and C/EBPα could induce hepatocytic characteristics, we introduced their cDNAs into mature cholangiocytes using retroviral vectors. Cholangiocytes induced with HNF4α or C/EBPα were sequentially treated with OSM and MG. Both HNF4α and C/EBPα slightly increased expression of albumin, whereas only C/EBPα upregulated *CPSI* (Fig. 3C).

Because the Notch signaling pathway has been implicated in cholangiocyte differentiation of hepatoblasts and hepatocytes (Tanimizu and Miyajima, 2004; Zong et al., 2009), we considered a possibility that constitutive activation of the pathway might inhibit hepatocytic differentiation of adult cholangiocytes. Therefore, we also examined whether inhibition of the Notch pathway by adding 3,5 difluorophenylacetyl L alanyl L 2 phenylglycine *t* butyl ester (DAPT), a γ secretase inhibitor that potentially blocks the Notch signaling pathway (Sastre et al., 2001), could induce the hepatocytic differentiation of mature cholangiocytes. The DAPT treatment slightly decreased expression of *Hes1*, one of major targets of the

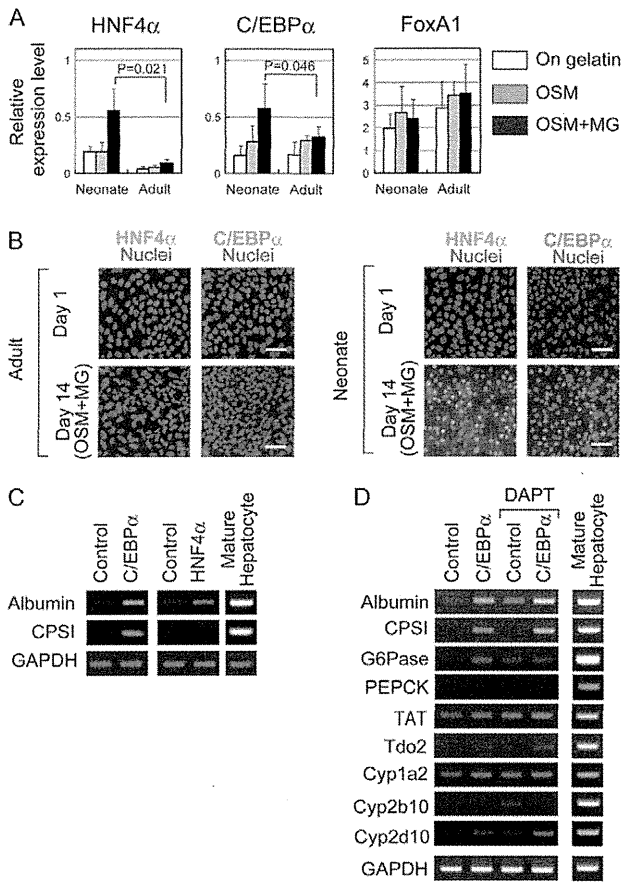

Fig. 3. Overexpression of C/EBPα slightly induces CPSI expression in adult cholangiocytes. (A) Expression of HNF4α, C/EBPα and FoxA1 in cholangiocytes during culture. HNF4α and C/EBPα were induced in neonatal cholangiocytes but not in adult cholangiocytes. FoxA1 was expressed in both types of cells. Expression levels are presented relative to the expression levels in MHs cultured for 1 day. Two-tailed Student's *t*-tests were performed using Microsoft Excel. (B) Protein expression of HNF4α and CPSI. HNF4α and C/EBPα proteins were induced in neonatal cholangiocytes after inducing hepatocytic differentiation. Nuclei were counterstained with Hoechst 33258. Scale bars: 50 μm. (C) Expression of CPSI was induced by the overexpression of C/EBPα, but not HNF4α. (D) Induction of hepatocyte markers by overexpression of C/EBPα in the presence of a γ-secretase inhibitor. Expression of albumin and CPSI hepatocytic induced by C/EBPα was further upregulated in the presence of DAPT, a γ-secretase inhibitor and a potent inhibitor for the Notch signaling pathway. The data also show that expression of Tdo2 and Cyp2d10 were slightly increased.

Notch pathway, whereas expression of albumin was significantly increased in the presence of DAPT (supplementary material Fig. S6).

Next, we examined whether overexpression of C/EBPα and inhibition of the Notch pathway have an additive effect on hepatocytic differentiation. As shown in Fig. 3D, albumin and *CPSI* were induced to a greater extent by a combination of DAPT and C/EBPα expression than by the treatment of either of them alone. *Tdo2* and *Cyp2d10* were slightly induced by the combination of DAPT with C/EBPα. Although the level of expression of hepatocyte markers was much lower than in MHs, C/EBPα expression affected the differentiation status of mature cholangiocytes.

Grainyhead-like 2 inhibits hepatocytic differentiation

Overexpression of C/EBPα only slightly promoted hepatocytic differentiation. Therefore, we assumed that molecular machinery strongly stabilizing the cholangiocyte lineage might exist in adult cholangiocytes. As candidates of inhibitory factors, we examined expression of cholangiocytic transcription factors including Sox9, hairy enhance of slit 1 (Hes1), Hey1 and grainyhead like 2 (Grhl2) that we identified as cholangiocyte specific transcription factors (Senga et al., 2012). Their expression was higher in adult cholangiocytes than in neonatal cells (Fig. 4A). Furthermore, Grhl2 and Hes1 were maintained at lower levels in neonatal cells than in adult cells during culture (Fig. 4B). Interestingly, Grhl2 expression was further inhibited in neonatal culture after inducing hepatocytic differentiation by sequential treatment with OSM and MG. Downregulation of Grhl2 in neonatal cholangiocytes and its continuous expression in adult cells during the culture were further confirmed by immunofluorescence analysis (supplementary material Fig. S7). Therefore, we considered the possibility that constant expression of Grhl2 in adult cholangiocytes might inhibit hepatocytic differentiation.

To test this hypothesis, we introduced Grhl2 into neonatal cholangiocytes and induced hepatocytic differentiation, and found that Grhl2 inhibited induction of hepatocyte markers (Fig. 4C). We further confirmed that Grhl2 blocked expression of albumin, CPSI, HNF4α, and C/EBPα proteins induced by OSM and MG (Fig. 4D). Moreover, the downregulation of Grhl2 by short interfering RNAs (siRNAs) in adult cholangiocytes slightly induced hepatocytic characteristics (supplementary material Fig. S8). These results suggest that maintenance of Grhl2 at a high level is a crucial factor fixing adult EpCAM^{+} cells in the cholangiocyte lineage.

Epithelial characteristics of neonatal and adult cholangiocytes

Given that Grhl2 is implicated in maturation of cholangiocytes (Senga et al., 2012), we considered the possibility that neonatal and adult cholangiocytes might be different in terms of their maturation status as epithelial cells, although bile duct structures are formed in neonatal liver (Fig. 5A). To examine epithelial characteristics of cholangiocytes, we cultured them to develop monolayers, and first measured transepithelial resistance (TER). In the culture condition used here, cholangiocytes formed a monolayer during 2 days of incubation. During and after the formation of the monolayers by neonatal and adult cholangiocytes, values of TER increased and reached a plateau (supplementary material Fig. S9). After 4 days of incubation, the monolayer of adult cholangiocytes showed the higher TER value than that of neonatal cells (Fig. 5B). We also examined the efflux of 4 kDa fluoresceinisothiocyanato dextran (FITC dextran) and found that FITC dextran passed through the monolayer derived from neonatal cholangiocytes more readily than through that of adult cells (Fig. 5C). These results indicated that neonatal

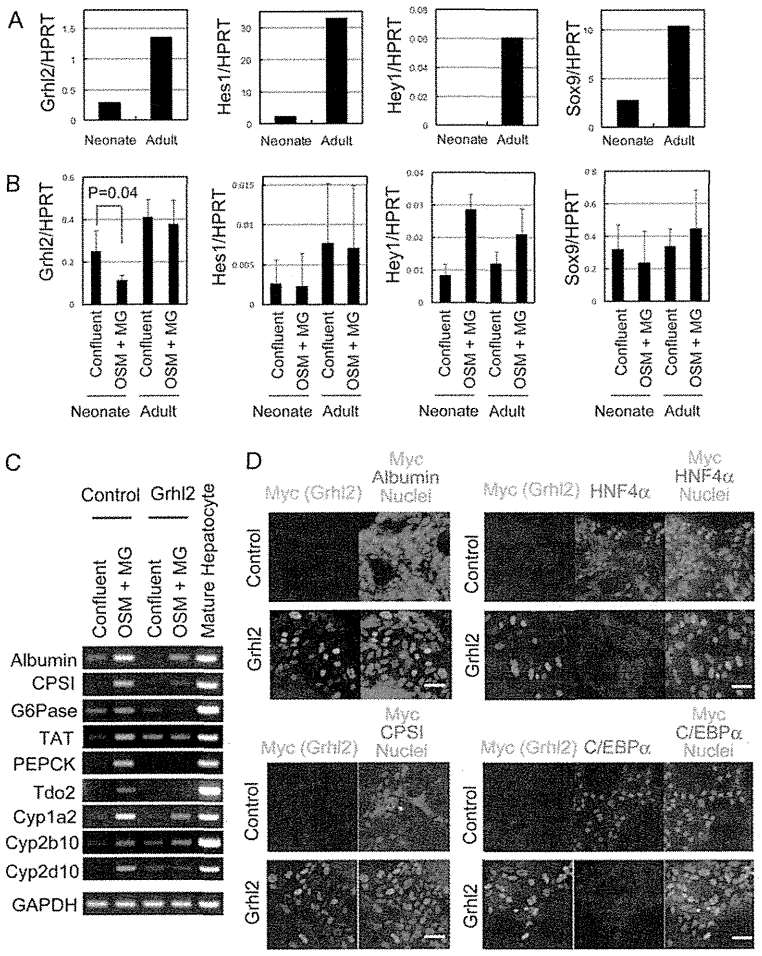

Fig. 4. Overexpression of Grhl2 inhibits hepatocyte conversion of neonatal cholangiocytes. (A) Cholangiocyte transcription factors are expressed more in neonatal cholangiocytes than in adult ones. Neonatal and adult cholangiocytes were isolated from 1W and 8W livers, respectively, as EpCAM^{+} cells by FACS. Expressions of Grhl2, Hes1, Hey1 and Sox9 were examined by quantitative PCR. Neonatal and adult cholangiocytes were isolated from six and three mice, respectively, as EpCAM^{+} cells by FACS. Cell isolation was repeated four times, independently. The expression levels are shown relative to that of adult cholangiocytes. (B) The expression of cholangiocyte transcription factors is changed during the culture of cholangiocytes. Expression of Grhl2 was downregulated in neonatal cholangiocytes during hepatocytic differentiation, whereas it was maintained in adult cells during culture. Expression of Hes1 in neonatal cholangiocytes remained at a lower level compared with adult cells. However, in contrast to Grhl2, Hes1 was not further downregulated during hepatocytic differentiation of neonatal cholangiocytes. Culture was repeated three times, independently. Error bars represent s.d. Two-tailed Student's *t*-tests were performed using Microsoft Excel. (C) Grhl2 inhibits hepatocytic differentiation of neonatal cholangiocytes. Grhl2 was introduced to neonatal cholangiocytes. Hepatocytic differentiation was induced by OSM and MG. Grhl2 inhibited the induction of hepatocytes markers. Cultures were repeated three times, independently. (D) Grhl2 inhibits expression of albumin, CPSI, HNF4α and C/EBPα proteins. Neonatal cholangiocytes introduced with the control vector or the vector containing Grhl2 were treated with OSM and MG. Expression of albumin, CPSI, HNF4α and C/EBPα was examined by immunostaining (red). Myc-tagged Grhl2 was detected by anti-Myc antibody (green). Scale bars: 50 μm.

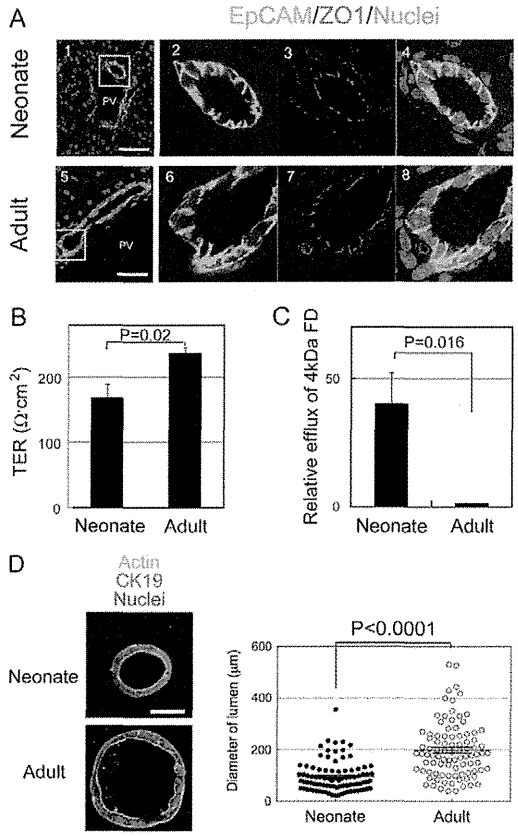

Fig. 5. Neonatal cholangiocytes are immature epithelial cells as compared with adult cells. (A) Bile ducts are present in neonatal and adult livers. EpCAM^{+} cholangiocytes form bile ducts in neonatal (1W-old) and adult livers. Tight junctions, recognized by ZO1 staining, are present around the lumens of neonatal and adult bile ducts. Liver sections were incubated with anti-EpCAM (green) and anti-ZO1 (red) antibodies. Nuclei were counterstained by Hoechst 33258. Boxes in panels 1 and 5 are enlarged in panels 2 4 and 6 8, respectively. Scale bars: 50 μm. (B) Neonatal cholangiocytes have a lower TER value. Fifty thousand cholangiocytes were plated onto Col-I gel in a 12-well plate. TER values at day 4 are shown in the graph. Cultures were repeated three times, independently. Bars indicate s.e.m. Two-tailed Student's *t*-tests were performed. (C) Higher paracellular efflux of 4 kDa FD occurs through the monolayer of neonatal cholangiocytes. At day 4 of culture, paracellular efflux of 4 kDa FITC-dextran (FD) was examined for the monolayers of neonatal and adult cholangiocytes. Bars indicate s.e.m. Two-tailed Student's *t*-tests were performed. (D) Neonatal cholangiocytes form smaller cysts than adult cells in 3D culture. Neonatal and adult cholangiocytes dissociated from Col-I gel were incubated in gel containing 5% Matrigel. Representative neonatal and adult cysts are shown in the left panels. Scale bar: 50 μm. After incubation for 10 days, the diameter of the lumen was measured. Cultures of neonatal and adult cholangiocytes were repeated three and two times, respectively. Each culture was performed in four wells. A dot plot is shown with bars indicating the means ± s.e.m.

cholangiocytes formed relatively immature tight junctions (TJs) compared with adult cells.

As we previously reported, maturation of TJs promotes epithelial morphogenesis, which could be correlated with enlargement of the apical lumen of cysts formed in three dimensional culture of epithelial cells (Senga et al., 2012). After 10 days of three dimensional culture, about 1% of neonatal and adult cholangiocytes formed cysts with a central lumen. However, the lumen size of neonatal cysts was significantly ($P<0.0001$) smaller than that of adult cysts, further suggesting that neonatal cells form relatively immature TJs compared with adult ones (Fig. 5D). These results indicate that neonatal cholangiocytes are immature epithelial cells.

Discussion

In this study, we demonstrated that cholangiocytes possess the ability to convert into hepatocytes in the neonatal period but this capability is lost in the adult. Similarly, it has been demonstrated that pancreatic duct cells have the potential to differentiate into endocrine and exocrine cells in the neonatal period but their differentiation potential becomes limited in the adult (Kopp et al., 2011). Thus, tubular epithelial cells may generally lose lineage plasticity during postnatal development.

Although, as we mentioned above, it has been shown that neonatal pancreatic duct cells lose the capability to differentiate to multiple types of cell during development, it is not known how the plasticity of epithelial cells is limited. We unexpectedly found that neonatal cholangiocytes are still developing epithelial characteristics even after forming the tubular structure. It can be assumed that production of bile by neonatal hepatocytes is less than that by mature ones and, therefore, relatively immature TJs in neonatal livers are sufficient to prevent the leakage of bile to the parenchyma and/or to the blood vessels, including the portal vein and the hepatic artery. This assumption seems to be consistent with the fact that the accumulation of bile in the neonatal gallbladder is much less than in the adult one (supplementary material Fig. S10). Furthermore, we showed that Grhl2 was expressed at a higher level in adult than in neonatal cholangiocytes and could inhibit hepatocytic differentiation. As we previously demonstrated, Grhl2 promotes formation of functional TJs by establishing a molecular network among claudin 3, claudin 4 and Rab25 (Senga et al., 2012). Thus, our results suggest that the molecular machinery that establishes the epithelial integrity limits the differentiation potential of epithelial cells and thereby stabilizes the lineage of the cells.

It was recently shown that transcription factors could covert fibroblasts into pluripotent stem cells or other types of somatic cells (Yamanaka and Blau, 2010; Yang, 2011). The combination of Gata4, HNF1α and FoxA1, or that of HNF4α plus FoxA1, A2 or A3, was able to convert mouse skin fibroblasts to hepatocytes (Huang et al., 2011; Sekiya and Suzuki, 2011). Because these proteins are strongly expressed in MHs but not in cholangiocytes, we considered the possibility that their expression status is a key to determining the potential for hepatocytic differentiation. In addition to these transcription factors, we focused on C/EBPα, which is also important for the functions of MHs (Inoue et al., 2004). During the course of hepatocytic differentiation, neonatal cholangiocytes expressed FoxA1, HNF4α and C/EBPα. Adult cholangiocytes, however, expressed FoxA1 but neither HNF4α nor C/EBPα. To elucidate the difference in induction, we examined epigenetic modification of the promoters of HNF4α and C/EBPα. Compared with hepatocytes, methylation of CpG sequences increased in cholangiocytes (supplementary material Fig. S11). However, there was little difference between 1W and 6W cholangiocytes. Other epigenetic mechanisms or upstream factors may regulate the expression of HNF4α and C/EBPα in hepatic epithelial cells. Although C/EBPα expression was effective in conferring hepatocytic characters on cholangiocytes,

the level of induction was limited. This indicates that other factors may block lineage conversion. The present study suggests that Grhl2 is one such inhibitory factor.

Although Grhl2 did not affect expression of C/EBPα mRNA, it did block induction of C/EBPα protein during hepatocytic differentiation (supplementary material Fig. S12; Fig. 4), suggesting that Grhl2 or its target inhibits translation of C/EBPα. However, downregulation of Grhl2 alone did not markedly induce expression of C/EBPα and hepatocytic differentiation in adult cholangiocytes. This result indicates that other molecules might be involved in regulating those processes. Nevertheless, when upregulation of C/EBPα and downregulation of Grhl2 simultaneously occurred in adult cholangiocytes, hepatocytic markers were further upregulated and some cells expressed albumin and CPSI proteins (supplementary material Fig. S13). Moreover, we demonstrated that the inhibition of the Notch pathway by DAPT was effective in inducing hepatocytic characteristics in adult cholangiocytes, although DAPT treatment only slightly upregulated Hes1. Given that the Notch pathway could regulate the lineage of hepatic epithelial cells independently of Hes1 (Jeliazkova et al., 2013), other targets of the pathway may be also involved in conferring hepatocytic characteristics in adult cholangiocytes. Taken together our results suggest that to induce hepatocytic differentiation in adult cholangiocytes, we may need to not only promote expression of hepatocytic transcription factors but also inhibit cholangiocytic factors and the Notch pathway.

In summary, we demonstrate here that cholangiocytes alter their lineage plasticity during epithelial maturation. We identified a possible molecular network augmenting epithelial structures and functions, which also contributes to stabilization of the epithelial cell lineage by blocking conversion to other lineages. Our results suggest that it is not easy to convert the mass of mature cholangiocytes to hepatocytes; however, several groups have reported that hepatocytes can be produced from pluripotent stem cells or somatic cells (Si Tayeb et al., 2010; Huang et al., 2011; Sekiya and Suzuki, 2011). Although induced hepatocytes differentiate to functional hepatocytes in diseased mice, it is still difficult to control the process of hepatocytic differentiation of pluripotent and somatic cells and produce a mass of MHs *in vitro*. Neonatal cholangiocytes have a remarkably strong ability to convert into hepatocytes, so for pluripotent cells to achieve the differentiation status of these cells would be an important step in the differentiation process. We have successfully expanded human cholangiocytes isolated from adult human liver tissue in the same culture conditions as used for mouse cholangiocytes (supplementary material Fig. S3). In addition, cholangiocytes isolated from extrahepatic bile ducts and the gallbladder of adult mice could proliferate efficiently in the same culture conditions (data not shown). Therefore, if we could find a factor that reverts mature cholangiocytes to the differentiation status of neonatal ones, it may be possible to produce functional hepatocytes that can be used as a source of cell therapy and for drug screening.

Materials and Methods

Extracellular matrix, growth factors and chemicals

Col-I (3 mg/ml) was purchased from Koken Co., Ltd (Tokyo, Japan). Growth factor-reduced Matrigel® (MG), which contains extracellular matrix proteins including type IV collagen, laminin-111 and nidogen, was purchased from BD Biosciences (Bedford, MA). Epidermal growth factor (EGF), hepatocyte growth factor (HGF) and OSM were purchased from R&D Systems (Minneapolis, MN).

Isolation and culture of cholangiocytes

One-week (1W)- and 6-week (6W)- old mice (C57BL6, Sankyo Lab Service, Japan) were used to isolate neonatal and adult cholangiocytes, respectively. All the animal experiments were approved by the Sapporo Medical University Institutional Animal Care and Use Committee and were carried out under the institutional guidelines for ethical animal use. A two-step collagenase perfusion method was performed through the portal vein of adult mice or through the left ventricle of neonatal mice to digest liver tissues. After the removal of parenchymal cells, the residual material including bile ducts was further digested with Liberase TM (Roche Applied Sciences, San Diego, CA) for neonatal tissues or with collagenase/hyaluronidase solution for adult tissues. Enzymatic digestion was terminated by adding ice-cold fresh medium containing 10% fetal bovine serum (FBS).

The cell suspension was passed sequentially through a 100-μm mesh and a 70-μm cell strainer (BD Biosciences). Nonspecific binding of antibodies was blocked by an antibody against the Fcγ receptor (anti-CD16/CD32 antibody; BD Biosciences). Cells were incubated with biotin-conjugated anti-EpCAM antibody (BioLegend, San Diego, CA) followed by streptavidin microbeads (Miltenyi Biotec, Gladbach, Germany). $EpCAM^+$ cells were purified through a MACS column (Miltenyi Biotec). Twenty thousand cells were placed in each well of a 12-well plate. For culture on Col-I gel or MG, collagen type IAC (Koken) mixed with 10× reconstitution buffer containing 200 mM HEPES, 50 mM NaOH, 260 mM $NaHCO_3$, 10× Dulbecco's modified Eagle's medium (DMEM) and PBS or MG was added to each well. To coat wells with collagen type IAC or MG, these agents were diluted in 0.1 M CH_3COOH and DMEM/F12 medium, respectively, and 500 μl of solution was added to each well. The cells were cultured in DMEM/F12 medium supplemented with 10% FBS, 10 ng/ml EGF and HGF, 5×10^{-8} M dexamethasone (Dex; Sigma Chemical Co., St. Louis, MO) and 1× insulin-transferrin-selenium (ITS; Gibco, Carlsbad, CA). After 5 7 days in culture, cells were dissociated from the dishes and then used for subculture (supplementary material Fig. S1).

Human liver tissue was obtained from a patient who underwent hepatic resection at Sapporo Medical University Hospital, with informed consent and the approval of the Sapporo Medical University Ethics Committees. The liver tissue was digested by a method reported previously (Sasaki et al., 2008). Cholangiocytes were isolated from the remaining tissue using the same protocol as that used for the isolation of mouse cholangiocytes and then purified through an MACS column with FITC-conjugated anti-human EpCAM (BioLegend) and anti-FITC microbeads (Miltenyi Biotec).

Induction of hepatocytic differentiation

After culture on Col-I gel, cholangiocytes were dissociated from the gel and 5×10^4 cells were cultured in each well of 24-well plates coated with gelatin. After the cells became confluent, they were incubated with 20 ng/ml OSM, 1% DMSO, 10^{-7} M Dex, and 1× ITS for 4 days and then overlaid with 5% MG for an additional 4 days.

To examine the ability to eliminate ammonium ions from the culture medium, NH_4Cl was added to the culture medium at 2 mM. The concentration of ammonium ions was measured every 2 hours by using the Ammonia Test Wako (Wako Pure Chemical Industries, Osaka, Japan).

To enhance the formation of bile canaliculus (BC) structures in the colonies, 100 μM taurocholate (Tokyo Chemical Industry Co. Ltd, Tokyo, Japan) was added to the medium for 1 day. The formation of BC-like structures was confirmed by incubation with 10 μg/ml fluorescein diacetate (FDA; Sigma-Aldrich, St. Louis, MO) for 30 minutes. The accumulation of metabolized fluorescein into BC-like structures was examined.

Overexpression of transcription factors

cDNAs of C/EBPα, HNF 4α and Grhl2 were amplified by PCR and inserted into retroviral vectors to generate pMXsNeo-C/EBPα, pMXsPuro-HNF4α and pMXsNeo-Grhl2. Retrovirus was added to the culture 48 hours after starting the culture on Col-I gel. For the control, pMXsNeo or pMXsPuro was introduced to cholangiocytes. G418 (1 mg/ml) or puromycin (10 μg/ml) was added to the culture 24 hours after infection to select cells with pMXsNeo-C/EBPα or pMXsNeo-Grhl2, and pMXsPuro-HNF4α, respectively. After incubation in the presence of antibiotics for 24 hours, cells were incubated in medium without them for 2 or 3 days before replating onto gelatin-coated dishes.

PCR

Total RNA was isolated from purified $EpCAM^+$ cells using an RNeasy Mini Kit (Qiagen, Hilden, Germany). cDNA was synthesized using an Omniscript Reverse Transcription Kit (Qiagen). Primers used for PCR are shown in supplementary material Table S1.

Immunofluorescence chemistry

Cholangiocytes induced to differentiate or colonies derived from $EpCAM^+$ cells were fixed in PBS containing 4% paraformaldehyde (PFA) at 4°C for 15 minutes.

After permeabilization with 0.2% Triton X-100 and blocking with Blockace (DS Pharma, Biomedical Co. Ltd, Osaka, Japan), cells were incubated with primary antibodies (supplementary material Table S2). Signals were visualized with Alexa-Fluor-488, -555 or -633-conjugated secondary antibodies (Molecular Probes, Carlsbad, CA). Nuclei were counterstained with Hoechst 33258. Images were acquired with a Nikon X-81 fluorescence microscope.

Measurement of TER and paracellular tracer flux

Fifty thousand cholangiocytes dissociated from the Col-I gel were replated on a 12 mm Transwell with a 0.4 μm pore, polyester membrane coated with Col-I gel, which was placed in a 12-well plate (Corning Inc., Corning, NY). TER was measured directly in the culture medium using a Millicell-ERS epithelial Volt Ohm meter (Millipore, Billerica, MA) during the culture. The TER values were calculated by subtracting the background TER of blank filters, followed by multiplying by the surface area of the filter (1.12 cm^2). For the paracellular tracer flux assay, 4 kDa FITC-dextran (Sigma-Aldrich) was added to the medium inside the Transwell dish on day 4 at a concentration of 1 mg/ml. After incubation for 2 hours, an aliquot of medium was collected from the basal compartment. The paracellular tracer flux was determined as the amount of FITC-dextran in the basal medium, which was measured with an Infinite M1000 Pro multi-plate reader (Tecan Group Ltd, Mannedorf, Switzerland).

Three-dimensional culture

Neonatal and adult cholangiocytes were cultured in gel containing Matrigel® as previously reported (Tanimizu et al., 2007). Briefly, cholangiocytes were dissociated from Col-I gel and 5,000 cells were replated on the mixture of Matrigel® and type I collagen (1:1 v/v) in a well of an 8-well coverglass chamber (Nunc, Roskilde, Denmark) covered with 5% Matrigel®. After 5 minutes of incubation, cells were fixed and used for immunofluorescence analysis.

Acknowledgements

We thank Ms Minako Kuwano and Ms Yumiko Tsukamoto for technical assistance.

Author contributions

N.T., study concept and design, acquisition and analysis of data, writing the manuscript, obtained funding; Y.N., sample preparation; N.I., discussion about data, T.M., sample preparation and obtained funding; K.H., obtained funding; T.M., editing the manucscript, obtained funding.

Funding

This work was supported by the Ministry of Education, Culture, Sports, Science and Technology, Japan, Grants in Aid for Young Scientists (B) [grant number 22790386 to N.T.]; Innovative Area [grant number 24112519 to N.T.]; and Grants in Aid for Scientific Research (B) [grant numbers 22390259 to K.H. and 21390365, 24390304 to T.M.].

Supplementary material available online at
http://jcs.biologists.org/lookup/suppl/doi:10.1242/jcs.133082/-/DC1

References

Espanol-Suner, R., Carpentier, R., Van Hul, N., Legry, V., Achouri, Y., Cordi, S., Jacquemin, P., Lemaigre, F. and Leclercq, I. A. (2012). Liver progenitor cells yield functional hepatocytes in response to chronic liver injury in mice. *Gastroenterology* **143**, 1564-1575, e1567.

Fu, D., Wakabayashi, Y., Lippincott-Schwartz, J. and Arias, I. M. (2011). Bile acid stimulates hepatocyte polarization through a cAMP-Epac-MEK-LKB1-AMPK pathway. *Proc. Natl. Acad. Sci. USA* **108**, 1403-1408.

Huang, P., He, Z., Ji, S., Sun, H., Xiang, D., Liu, C., Hu, Y., Wang, X. and Hui, L. (2011). Induction of functional hepatocyte-like cells from mouse fibroblasts by defined factors. *Nature* **475**, 386-389.

Inoue, Y., Inoue, J., Lambert, G., Yim, S. H. and Gonzalez, F. J. (2004). Disruption of hepatic C/EBPalpha results in impaired glucose tolerance and age-dependent hepatosteatosis. *J. Biol. Chem.* **279**, 44740-44748.

Jeliazkova, P., Jors, S., Lee, M., Zimber-Strobl, U., Ferrer, J., Schmid, R. M., Siveke, J. T. and Geisler, F. (2013). Canonical Notch2 signaling determines biliary cell fates of embryonic hepatoblasts and adult hepatocytes independent of Hes1. *Hepatology* **57**, 2469-2479.

Kopp, J. L., Dubois, C. L., Hao, E., Thorel, F., Herrera, P. L. and Sander, M. (2011). Progenitor cell domains in the developing and adult pancreas. *Cell Cycle* **10**, 1921-1927.

Mackey, S. L. and Darlington, G. J. (2004). CCAAT enhancer-binding protein alpha is required for interleukin-6 receptor alpha signaling in newborn hepatocytes. *J. Biol. Chem.* **279**, 16206-16213.

Malato, Y., Naqvi, S., Schürmann, N., Ng, R., Wang, B., Zape, J., Kay, M. A., Grimm, D. and Willenbring, H. (2011). Fate tracing of mature hepatocytes in mouse liver homeostasis and regeneration. *J. Clin. Invest.* **121**, 4850-4860.

Michalopoulos, G. K. (2007). Liver regeneration. *J. Cell. Physiol.* **213**, 286-300.

Michalopoulos, G. K. (2011). Liver regeneration: alternative epithelial pathways. *Int. J. Biochem. Cell Biol.* **43**, 173-179.

Nishikawa, Y., Doi, Y., Watanabe, H., Tokairin, T., Omori, Y., Su, M., Yoshioka, T. and Enomoto, K. (2005). Transdifferentiation of mature rat hepatocytes into bile duct-like cells in vitro. *Am. J. Pathol.* **166**, 1077-1088.

Oertel, M., Rosencrantz, R., Chen, Y. Q., Thota, P. N., Sandhu, J. S., Dabeva, M. D., Pacchia, A. L., Adelson, M. E., Dougherty, J. P. and Shafritz, D. A. (2003). Repopulation of rat liver by fetal hepatoblasts and adult hepatocytes transduced ex vivo with lentiviral vectors. *Hepatology* **37**, 994-1005.

Parviz, F., Matullo, C., Garrison, W. D., Savatski, L., Adamson, J. W., Ning, G., Kaestner, K. H., Rossi, J. M., Zaret, K. S. and Duncan, S. A. (2003). Hepatocyte nuclear factor 4alpha controls the development of a hepatic epithelium and liver morphogenesis. *Nat. Genet.* **34**, 292-296.

Sasaki, K., Kon, J., Mizuguchi, T., Chen, Q., Ooe, H., Oshima, H., Hirata, K. and Mitaka, T. (2008). Proliferation of hepatocyte progenitor cells isolated from adult human livers in serum-free medium. *Cell Transplant.* **17**, 1221-1230.

Sastre, M., Steiner, H., Fuchs, K., Capell, A., Multhaup, G., Condron, M. M., Teplow, D. B. and Haass, C. (2001). Presenilin-dependent gamma-secretase processing of beta-amyloid precursor protein at a site corresponding to the S3 cleavage of Notch. *EMBO Rep.* **2**, 835-841.

Sekine, K., Chen, Y. R., Kojima, N., Ogata, K., Fukamizu, A. and Miyajima, A. (2007). Foxo1 links insulin signaling to C/EBPalpha and regulates gluconeogenesis during liver development. *EMBO J.* **26**, 3067-3615.

Sekiya, S. and Suzuki, A. (2011). Direct conversion of mouse fibroblasts to hepatocyte-like cells by defined factors. *Nature* **475**, 390-393.

Sekiya, T., Muthurajan, U. M., Luger, K., Tulin, A. V. and Zaret, K. S. (2009). Nucleosome-binding affinity as a primary determinant of the nuclear mobility of the pioneer transcription factor FoxA. *Genes Dev.* **23**, 804-809.

Senga, K., Mostov, K. E., Mitaka, T., Miyajima, A. and Tanimizu, N. (2012). Grainyhead-like 2 regulates epithelial morphogenesis by establishing functional tight junctions through the organization of a molecular network among claudin3, claudin4, and Rab25. *Mol. Biol. Cell* **23**, 2845-2855.

Si-Tayeb, K., Noto, F. K., Nagaoka, M., Li, J., Battle, M. A., Duris, C., North, P. E., Dalton, S. and Duncan, S. A. (2010). Highly efficient generation of human hepatocyte-like cells from induced pluripotent stem cells. *Hepatology* **51**, 297-305.

Tanimizu, N. and Miyajima, A. (2004). Notch signaling controls hepatoblast differentiation by altering the expression of liver-enriched transcription factors. *J. Cell Sci.* **117**, 3165-3174.

Tanimizu, N., Nishikawa, M., Saito, H., Tsujimura, T. and Miyajima, A. (2003). Isolation of hepatoblasts based on the expression of Dlk/Pref-1. *J. Cell Sci.* **116**, 1775-1786.

Tanimizu, N., Miyajima, A. and Mostov, K. E. (2007). Liver progenitor cells develop cholangiocyte-type epithelial polarity in three-dimensional culture. *Mol. Biol. Cell* **18**, 1472-1479.

Yamanaka, S. and Blau, H. M. (2010). Nuclear reprogramming to a pluripotent state by three approaches. *Nature* **465**, 704-712.

Yamasaki, H., Sada, A., Iwata, T., Niwa, T., Tomizawa, M., Xanthopoulos, K. G., Koike, T. and Shiojiri, N. (2006). Suppression of C/EBPalpha expression in periportal hepatoblasts may stimulate biliary cell differentiation through increased Hnf6 and Hnf1b expression. *Development* **133**, 4233-4243.

Yang, L. (2011). From fibroblast cells to cardiomyocytes: direct lineage reprogramming. *Stem Cell Res. Ther.* **2**, 1.

Zong, Y., Panikkar, A., Xu, J., Antoniou, A., Raynaud, P., Lemaigre, F. and Stanger, B. Z. (2009). Notch signaling controls liver development by regulating biliary differentiation. *Development* **136**, 1727-1739.

HEPATOLOGY
Official Journal of the American Association for the Study of Liver Diseases

Differentiation Capacity of Hepatic Stem/Progenitor Cells Isolated From D-Galactosamine-Treated Rat Livers

Norihisa Ichinohe,[1] Naoki Tanimizu,[1] Hidekazu Ooe,[1] Yukio Nakamura,[1,2] Toru Mizuguchi,[2] Junko Kon,[1] Koichi Hirata,[2] and Toshihiro Mitaka[1]

Oval cells and small hepatocytes (SHs) are known to be hepatic stem and progenitor cells. Although oval cells are believed to differentiate into mature hepatocytes (MHs) through SHs, the details of their differentiation process are not well understood. Furthermore, it is not certain whether the induced cells possess fully mature functions as MHs. In the present experiment, we used Thy1 and CD44 to isolate oval and progenitor cells, respectively, from D-galactosamine-treated rat livers. Epidermal growth factor, basic fibroblast growth factor, or hepatocyte growth factor could trigger the hepatocytic differentiation of sorted $Thy1^+$ cells to form epithelial cell colonies, and the combination of the factors stimulated the emergence and expansion of the colonies. Cells in the $Thy1^+$-derived colonies grew more slowly than those in the $CD44^+$-derived ones *in vitro* and *in vivo* and the degree of their hepatocytic differentiation increased with CD44 expression. Although the induced hepatocytes derived from $Thy1^+$ and $CD44^+$ cells showed similar morphology to MHs and formed organoids from the colonies similar to those from SHs, many hepatic differentiated functions of the induced hepatocytes were less well performed than those of mature SHs derived from the healthy liver. The gene expression of cytochrome P450 1A2, tryptophan 2,3-dioxygenase, and carbamoylphosphate synthetase I was lower in the induced hepatocytes than in mature SHs. In addition, the protein expression of CCAAT/enhancer-binding protein alpha and bile canalicular formation could not reach the levels of production of mature SHs. *Conclusion*: The results suggest that, although $Thy1^+$ and $CD44^+$ cells are able to differentiate into hepatocytes, the degree of maturation of the induced hepatocytes may not be equal to that of healthy resident hepatocytes. (HEPATOLOGY 2012; 57:1192-1202)

The liver normally exhibits a very low level of cell turnover, but when loss of mature hepatocytes (MHs) occurs, a rapid regenerative response is elicited from all cell types in the liver to restore the organ to its initial state. The loss may occur as a result of toxic injury, viral infection, trauma, or surgical resection. Because hepatocytes are the major functional cells of the liver, large-scale hepatocytic loss becomes a trigger for regeneration, and replication of existing hepatocytes is generally the quickest, most efficient way to compensate for the lost functions. However, when the replication of hepatocytes is delayed or entirely inhibited, hepatic stem/progenitor cells (HPCs) are activated.[1-3] As HPCs, oval cells and small hepatocytes (SHs) are well known. Oval cells were first reported to be cells that possessed an ovoid nucleus and

Abbreviations: Abs, antibodies; AFP, alpha-fetoprotein; Alb, albumin; BC, bile canaliculus; bFGF, basic fibroblast growth factor; BrdU, 5-bromo-2'-deoxyuridine; BW, body weight; CPS-I, carbamoylphosphate synthetase I; CK, cytokeratin; C/EBP, CCAAT/enhancer-binding protein; CYP1A2, cytochrome P450 1A2; 3D, three-dimensional; DPPIV, dipeptidylpeptidase IV; ECM, extracellular matrix; EGF, epidermal growth factor; FD, fluorescent diacetate; FGF, fibroblast growth factor; GalN, D-galactosamine; HA, hyaluronic acid; HGF, hepatocyte growth factor; HNF, hepatocyte nuclear factor; HPCs, hepatic stem/progenitor cells; ICC, immunocytochemistry; INF-γ, interferon-gamma; IP, intraperitoneally; LI, labeling index; MH, mature hepatocyte; mRNA, messenger RNA; PBS, phosphate-buffered saline; PH, partial hepatectomy; qPCR, quantitative polymerase chain reaction; RET, retrorsine; SH, small hepatocyte; TAT, tyrosine aminotransferase; TGF, transforming growth factor; TNF-α, tumor necrosis factor alpha; TDO, tryptophan 2,3-dioxygenase;

From the [1]Department of Tissue Development and Regeneration, the Research Institute for Frontier Medicine, and [2]First Department of Surgery, Sapporo Medical University School of Medicine, Sapporo, Japan.

Received January 31, 2012; accepted September 8, 2012.

This work was supported by the Ministry of Education, Culture, Sports, Science, and Technology, Japan, Grant-in-Aid for Scientific Research (C) (19566021; to N.I.), Grants-in-Aid for Young Scientists (B) (22790385, to N.I.; and 19790294, to J.K.), a grant from the Yuasa Memorial Foundation (to T.M.), and Grants-in-Aid for Scientific Research (B) (22390259, to K.H.; and 21390365, to T.M.), a program for developing the supporting system for upgrading the education and research (to T.M.).

Dr. Kon is currently affiliated with Gene Techno Science Co. Ltd., Sapporo, Japan.

scant cytoplasm.[4] The appearance of oval cells has been reported in rat livers treated with hepatotoxins, such as 2-acetylaminofluorene (2-AAF), combined with partial hepatectomy (PH) and D-galactosamine (GalN).[1,5–7] In GalN-induced rat liver injury, it has been shown that oval cells appear in the periportal area and differentiate into MHs through basophilic small-sized ones.[8,9] Oval cells show a wide range of phenotypic heterogeneity, and cytokeratins (CKs) 7 and 19, alpha-fetoprotein (AFP), CD34, c-kit, and Thy1 have been reported as markers for them.[1,2,5–7]

On the other hand, SHs are a subpopulation of hepatocytes, and cells isolated from healthy adult rats[10,11] and human livers[12] can clonally proliferate to form colonies and differentiate into MHs *in vitro*.[11,13] Recently, we identified CD44 as a specific marker of SHs.[14] In GalN-treated rat livers, $CD44^+$ cells appear near the periportal area between $Thy1^+$ oval cells and resident hepatocytes soon after the emergence of $Thy1^+$ oval cells.[15] In addition, we previously showed that $Thy1^+$ oval cells differentiate into hepatocytes through $CD44^+$ cells.[15,16] Our data suggested that cells sequentially converted from $Thy1^+CD44^-$ to $Thy1^+CD44^+$ and then to $Thy1^-CD44^+$ cells during the process of hepatocytic differentiation of oval cells.[15,16] Furthermore, sorted $Thy1^+$ and $CD44^+$ cells could repopulate host livers when they were transplanted into rat livers treated with retrorsine (RET) and two-thirds PH.

Although most oval cells are thought to differentiate into MHs, the details of their differentiation process, such as factors for hepatic commitment, characteristics of intermediate cells, and their fates are not well understood. In addition, it has not been elucidated whether the induced hepatocytes differentiate to possess the same capabilities as MHs. In the present experiment, we aimed to clarify which factors might induce hepatocytic differentiation of $Thy1^+$ cells and to examine how $Thy1^+$ cells could differentiate into hepatocytes through $CD44^+$ cells. In addition, we examined whether the $Thy1^+$ and $CD44^+$ cells could differentiate into fully MHs, as with those in the healthy adult liver.

Materials and Methods

Animals and Liver Injury Model. Male F344 rats (dipeptidylpeptidase IV $[DPPIV]^+$ strain; Sankyo Lab Service Corporation, Inc., Tokyo, Japan), weighing 150-200 g, were used. All animals received humane care, and the experimental protocol was approved by the committee on laboratory animals according to Sapporo Medical University guidelines. For GalN-injured livers, GalN (75 mg/100 g body weight [BW] dissolved in phosphate-buffered saline [PBS]; Acros, Geel, Belgium) was intraperitoneally (IP) administered.[14] For the transplantation experiment, female F344 rats (DPPIV strain; Charles River Laboratories, Wilmington, MA) were (IP) given two injections of RET (30 mg/kg BW; Sigma-Aldrich Chemical Co., St. Louis, MO), 2 weeks apart,[17] and 4 weeks after the second injection, two-thirds PH was performed (RET/PH liver). Sorted $DPPIV^+$ cells (5×10^5 cells/0.5 mL) were transplanted into RET/PH livers (DPPIV) through the spleen (at least 3 rats per group).

Isolation and Culture of Cells. Rats were used to isolate hepatic cells by the collagenase perfusion method, as previously described.[18] After perfusion, the cell suspension was centrifuged at $50 \times g$ for 1 minute. The supernatant and the precipitate were used for sorting $Thy1^+$ and $CD44^+$ cells and preparing MHs, respectively. The procedure used for cell sorting was as previously described,[15] with some modifications. Antibodies (Abs) used for cell sorting are listed in Supporting Table 1. $Thy1^+CD44^+$ cells were sorted from $CD44^+$ cell and $Thy1^+$ cell fractions by using anti-Thy1 or CD44 Abs, respectively, and both were pooled. Furthermore, $Thy1^+$ and $CD44^+$ cells were also separated from CD44 and Thy1 cell fractions, respectively. After the number of viable cells was counted, 1×10^5 viable cells were plated in 12-well plates (Corning Inc., Corning, NY) and cultured in the medium listed in Supporting Table 2. The medium was replaced with fresh medium thrice-weekly.

To examine whether cells in the colonies could fully differentiate into MHs and form functional bile canaliculi (BCs), $Thy1^+CD44^-$ and $Thy1^-CD44^+$ cells sorted from GalN-D3 and SHs derived from a healthy liver were cultured for 10 days. Thereafter, some dishes were treated with Matrigel (BD Biosciences, San Diego, CA) for 10 days. To enhance the organoid formation of the colonies, as previously reported,[19]

Address reprint requests to: Norihisa Ichinohe, D.D.S., Ph.D., Department of Tissue Development and Regeneration, Research Institute for Frontier Medicine, Sapporo Medical University School of Medicine, South-1, West-17, Chuo-ku, Sapporo 060-8556, Japan. E-mail: nichi@sapmed.ac.jp; fax: +81-11-615-3099.

View this article online at wileyonlinelibrary.com.
DOI 10.1002/hep.26084
Potential conflict of interest: Nothing to report.
Additional Supporting Information may be found in the online version of this article.

colonies were separated from dishes by using Cell Dissociation Solution (Sigma-Aldrich), and colonies (2×10^3) were replated on collagen-coated dishes. Cells were cultured in the induction medium (Supporting Table 2) for 14 days. Cloning rings were used to isolate total RNA of each colony. At least two separate experiments were performed, and more than five colonies were investigated.

GeneChip Analysis, RNA Isolation, and Real-Time Polymerase Chain Reaction. Details are shown in the Supplementary Methods.

Immunostaining. For detecting $CD44^+$ colonies, cells were fixed with cold absolute ethanol at 10 days after plating, and immunocytochemistry (ICC) for CD44 was carried out. Details of staining were previously reported.[15] The numbers of $CD44^+$ colonies at days 5 and 10 were counted, and positivity was calculated. Three separate experiments were performed. To measure the labeling index (LI), 40 μM of 5-bromo-2'-deoxyuridine (BrdU) were added to the medium 24 hours before fixation. In double ICC for CD44 and BrdU, a combination of the avidin-biotin peroxidase complex method (Vectastain ABC Elite Kit; Vector Laboratories Inc., Burlingame, CA) and the alkaline phosphatase method was used. For fluorescent immunohistochemistry, sliced liver samples were frozen using isopentane/liquid nitrogen, and materials were kept at 80°C until use. All Abs used for immunostaining are listed in Supporting Table 1. Sections were embedded with 90% glycerol including 0.01% *p*-phenylenediamine and 4,6-diamidino-2-phenylindole. A confocal laser microscope (Olympus, Tokyo, Japan) was used for observation, and findings were analyzed using DP Manager (Olympus).

Treatment With Fluorescein Diacetate. As previously reported,[20] fluorescein diacetate (FD; Sigma-Aldrich) was dissolved in dimethyl sulfoxide, and the solution was diluted with the culture medium. Then, 0.25% FD was added to the medium, and the dish was rinsed three times with warm PBS. Fluorescent images were immediately photographed using a phase-contrast microscope equipped with a fluorescence device (Olympus).

Enzyme Histochemisty for DPPIV. To identify donor cells, enzyme histochemistry for DPPIV was carried out. DPPIV enzyme activity was detected as previously described.[15] $DPPIV^+$ foci in livers were photographed using a microscope equipped with a CCD camera, and the area of each focus was measured using ImageJ software (http://rsb.info.nih.gov/ij/index.html).

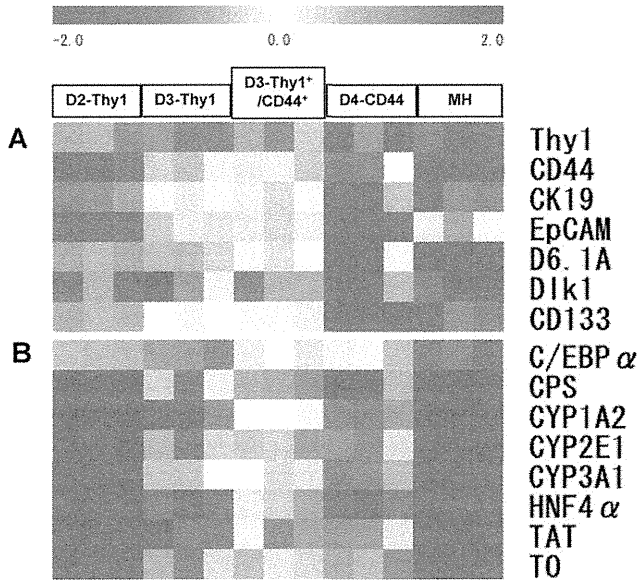

Fig. 1. Gene expression of sorted GalN-D2-$Thy1^+$ cells, D3-$Thy1^+$ cells, D3- $Thy1^+/CD44^+$ cells, and D4-$CD44^+$ cells. The gene-expression pattern of sorted cells was analyzed using GeneChip (Affymetrix, Inc., Santa Clara, CA). MHs isolated from a healthy adult rat liver were used as a control. A heatmap for genes that are classified into (A) stem cell and HPC markers and (B) hepatic markers. Relative expression of genes is shown in $\log_2$ scale. Increases in mRNA level are represented as shades of red and decreases as shades of blue.

Statistical Analysis. All data were analyzed using Turkey-Kramer's multiple comparison test. Level of statistical significance was $P < 0.05$. Experimental results are expressed as the geometric mean ± standard deviation.

Results

Characterization of Isolated Cells From Livers Treated by GalN. As previously reported,[15] $Thy1^+$ cells differentiated into hepatocytes through a $CD44^+$ intermediate state, as shown with clonally cultured $Thy1^+$ cells and cell transplantation. This transition likely happened in the GalN-treated rat liver as well. GeneChip data (Affymetrix, Inc., Santa Clara, CA) indicated that the immature hepatocyte markers, Dlk[21] and AFP were up-regulated in $Thy1^+CD44^+$ and Thy1 $CD44^+$ cells, whereas markers related to hepatic differentiation were gradually up-regulated during the transition from Thy1-D2 to CD44-D4 cells (Fig. 1). The results also suggested that most D2-$Thy1^+$ cells were not committed to the hepatic lineage. This is consistent with our previous finding that $Thy1^+$ cells isolated from GalN-D2 could form a few epithelial cell colonies in the standard medium for SH induction, whereas those from GalN-D3 certainly formed colonies consisting of $CD44^+$ cells. Therefore, we

Table 1. Effects of Growth Factors and Cytokines on the Formation of Epithelial Cell Colonies

Growth Factors	Numbers of Colonies/Well	Numbers of Cells/Colony
Control	0	0
EGF	4.5 ± 3.8	41.4 ± 1.8
bFGF	0.3 ± 0.6	13.0 ± 0.0
HGF	1.0 ± 1.7	24.6 ± 11.7
LIF	0	0
TNF α	0	0
IFN γ	0	0
OSM	0	0
PDGF BB	0	0
SCF	0	0
IL 6	0	0
TGF β1	0	0
TGF β2	0	0

Abbreviations: LIF, leukemia inhibitory factor; OSM, oncostatin M; PDGF BB, plate let derived growth factor BB; SCF, stem cell factor.

considered the possibility that Thy1$^+$ cells became the hepatocyte lineage between D2 and D3. To specify the factors that trigger hepatic commitment, we compared expression patterns of genes related to receptors of growth factors and cytokines and selected 12 candidates (Table 1).

Induction of Epithelial Cell Colonies by Growth Factors. D2-Thy1$^+$ cells were cultured in the medium supplemented with each factor. To elucidate the formation of epithelial cell colonies, ICC for CD44 was conducted 10 days after plating. Of the 12 candidates, only epidermal growth factor (EGF), basic fibroblast growth factor (bFGF), and hepatocyte growth factor (HGF) could induce colonies (Fig. 2A; Table 1). CD44 expression of cells varied among the colonies, and some colonies consisted of cells with low expression of CD44 (CD44 cells). Next, we examined whether bFGF and/or HGF could enhance the formation and expansion of colonies in the culture with EGF (Fig. 2B). Compared to EGF only (control), the addition of bFGF or HGF did not enhance the frequency of colony formation. In the combination of EGF and bFGF or HGF, the number of cells per colony increased to twice as many as in the control (Fig. 2C). In addition, the combination of the three factors also dose dependently increased the number of cells per colony. These results suggested that a certain number of Thy1$^+$ cells possessed the ability to differentiate into hepatic cells, and that the induction was initiated by EGF, bFGF, and/or HGF.

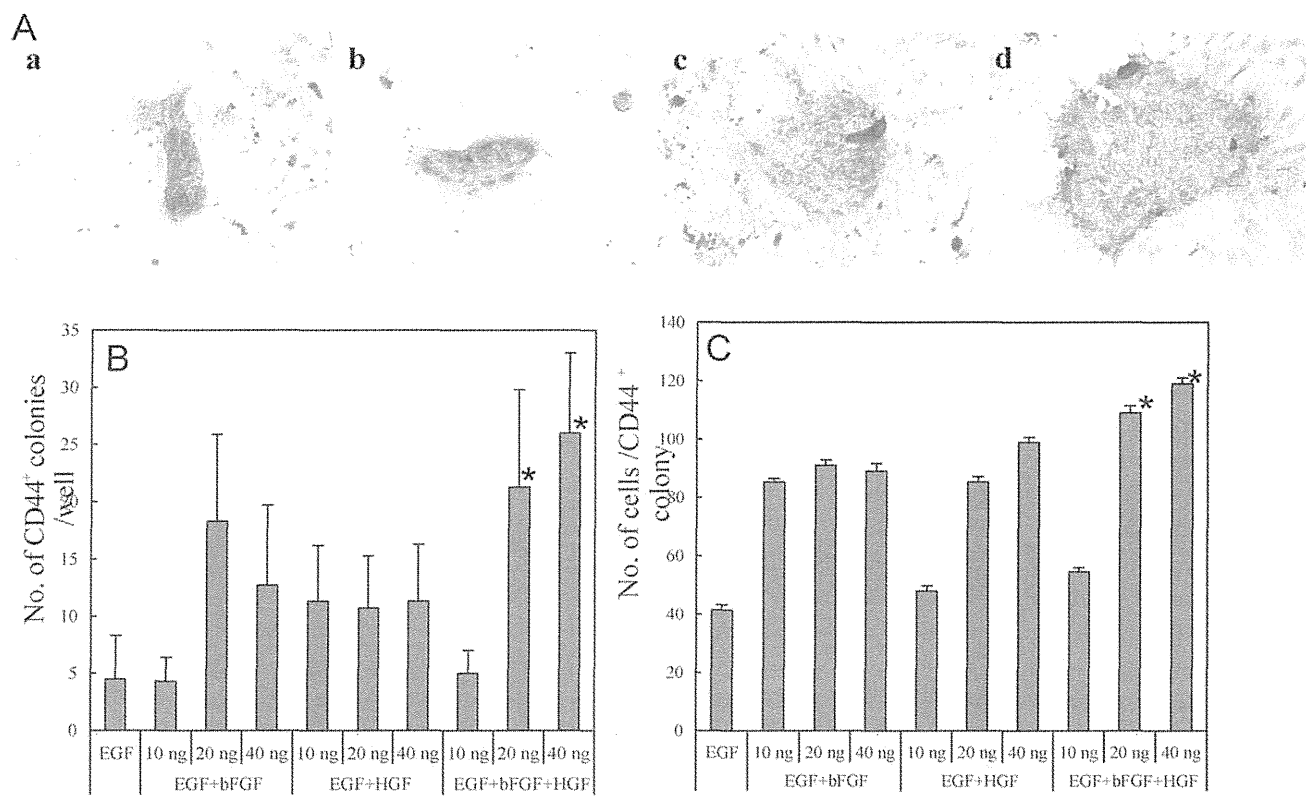

Fig. 2. Induction of CD44-positive cell colonies from sorted D2-Thy1$^+$ cells by treatment with EGF, bFGF, and/or HGF. Thy1$^+$ cells (1×10^5 viable cells/well) sorted from the GalN-D2 liver were plated on 12-well plates and cultured in medium supplemented with EGF (a), EGF+bFGF (b), EGF+HGF (c), and EGF+bFGF+HGF (d) for 10 days. Dose dependency of colony formation was examined. To identify colonies, ICC for CD44 was carried out. The number of CD44$^+$ cell colonies per well (B) and that of cells per colony (C) were measured. Asterisks shown in (B) and (C) indicate significance: $P < 0.05$, compared to EGF and 10 ng of EGF+bFGF+HGF.

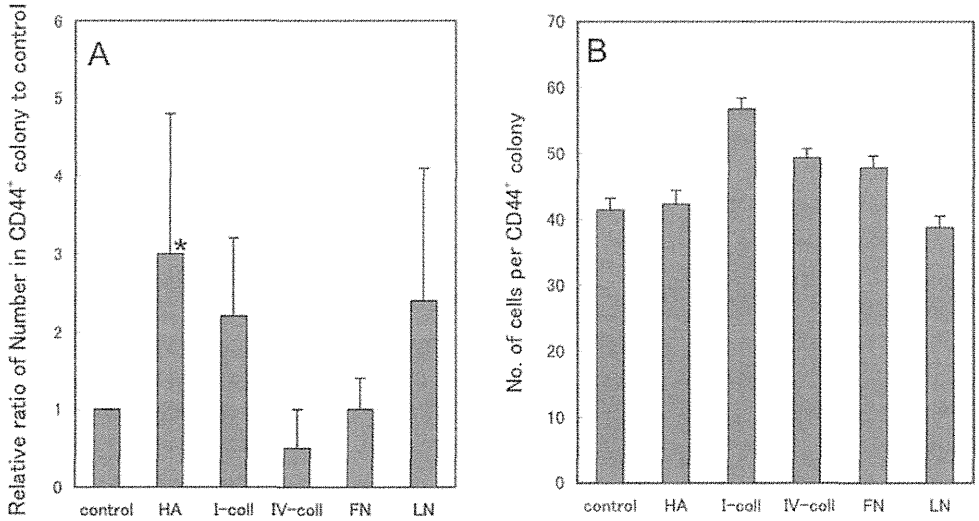

Fig. 3. Effects of ECM on colony formation of Thy1$^+$ cells were investigated. Thy1$^+$ cells were isolated from GalN-D2 rat livers and plated on dishes coated with hyaluronic acid (HA), type I collagen (I-coll), type IV collagen (IV-coll), fibronectin (FN), and laminin (LN). Noncoated dishes were used as controls. Cells were cultured in medium with EGF. To identify the colony, ICC for CD44 was carried out. The number of CD44$^+$ cell colonies per dish (A) and that of cells per colony (B) were measured. Asterisk shows significance: $P < 0.05$, control versus HA.

Induction of Epithelial Cell Colonies by Extracellular Matrix. Because CD44 is one of the receptors of hyaluronic acid (HA)[22,23] and because SHs can selectively proliferate on HA,[18] we investigated whether extracellular matrix (ECM) affected the frequency of emergence and phenotype of colonies derived from D2-Thy1$^+$ cells. Sorted D2-Thy1$^+$ cells were cultured on dishes coated with type I collagen, fibronectin, laminin, and HA, and ICC for CD44 was performed 10 days after plating. When cells were cultured in the medium supplemented with EGF, frequency of colony formation was significantly higher for cells on HA-coated dishes than for the control (Fig. 3A), but no difference was observed in the number of cells per colony among the dishes with each ECM (Fig. 3B).

Growth Ability and CD44 Expression of Cells Sorted From GalN-D3. Thy1$^+$CD44 (Thy1), Thy1$^+$CD44$^+$, and Thy1 CD44$^+$ (CD44) cells sorted from a GalN-D3 liver were cultured in the medium with EGF for 10 days. Double ICC for CD44 and BrdU was carried out (Fig. 4A–C). The frequency of colony formation was more than four times higher for CD44 cells than for both Thy1 and Thy1$^+$CD44$^+$ cells (Fig. 4D), and the average number of cells per colony was significantly larger for CD44 cells than for Thy1 and Thy1$^+$CD44$^+$ cells (Fig. 4E). The percentages of BrdU$^+$ cells were approximately 70% and 80% in colonies derived from Thy1 and CD44 cells, respectively (Fig. 4A–C, F). Growth ability of Thy1$^+$CD44$^+$ cells was also intermediate between those of Thy1 and CD44 cells.

Intensity and the localization of CD44 varied among cells forming colonies. In spite of the origin of sorted cells, CD44 protein was usually expressed in cell membranes between cells (Fig. 4C). Some colonies consisted of cells with CD44 protein localized in both the cell membrane and cytoplasm (Fig. 4A, B). The latter type of colony was often observed in the culture of Thy1 cells. CD44 positivity of Thy1$^+$ cells in a colony was approximately 65% at day 5 and increased to approximately 80% at day 10 (Fig. 4G).

Next, to examine whether acquisition of CD44 expression in Thy1$^+$ cells was also correlated to growth ability of cells *in vivo*, cell transplantation was carried out. D2-Thy1$^+$, D3-Thy1$^+$CD44$^-$, D3-Thy1$^+$CD44$^+$, D3-Thy1 CD44$^+$, and D4-CD44$^+$ cells (5×10^5 cells/rat) isolated from GalN-treated livers were intrasplenically transplanted into RET/PH-treated rats. One month after transplantation, the number of cells in foci derived from D4-CD44 was much larger than in those from Thy1-expressing cells (Fig. 4H, I). The growth rate of engrafted cells increased in correlation with the expression of CD44 and time after GalN treatment. In addition, no types of donor-derived (Y chromosome$^+$) cells, other than hepatocytes, could be found in recipient livers (Supporting Fig. 1).

Gene Expression of Hepatic Markers of Epithelial Cell Colonies Derived From D3-Thy1 Cells. To elucidate the characteristics of cells in colonies derived from D3-Thy1 cells, quantitative polymerase chain reaction (qPCR) of cells was performed for each colony, which was separated from the culture dish using a

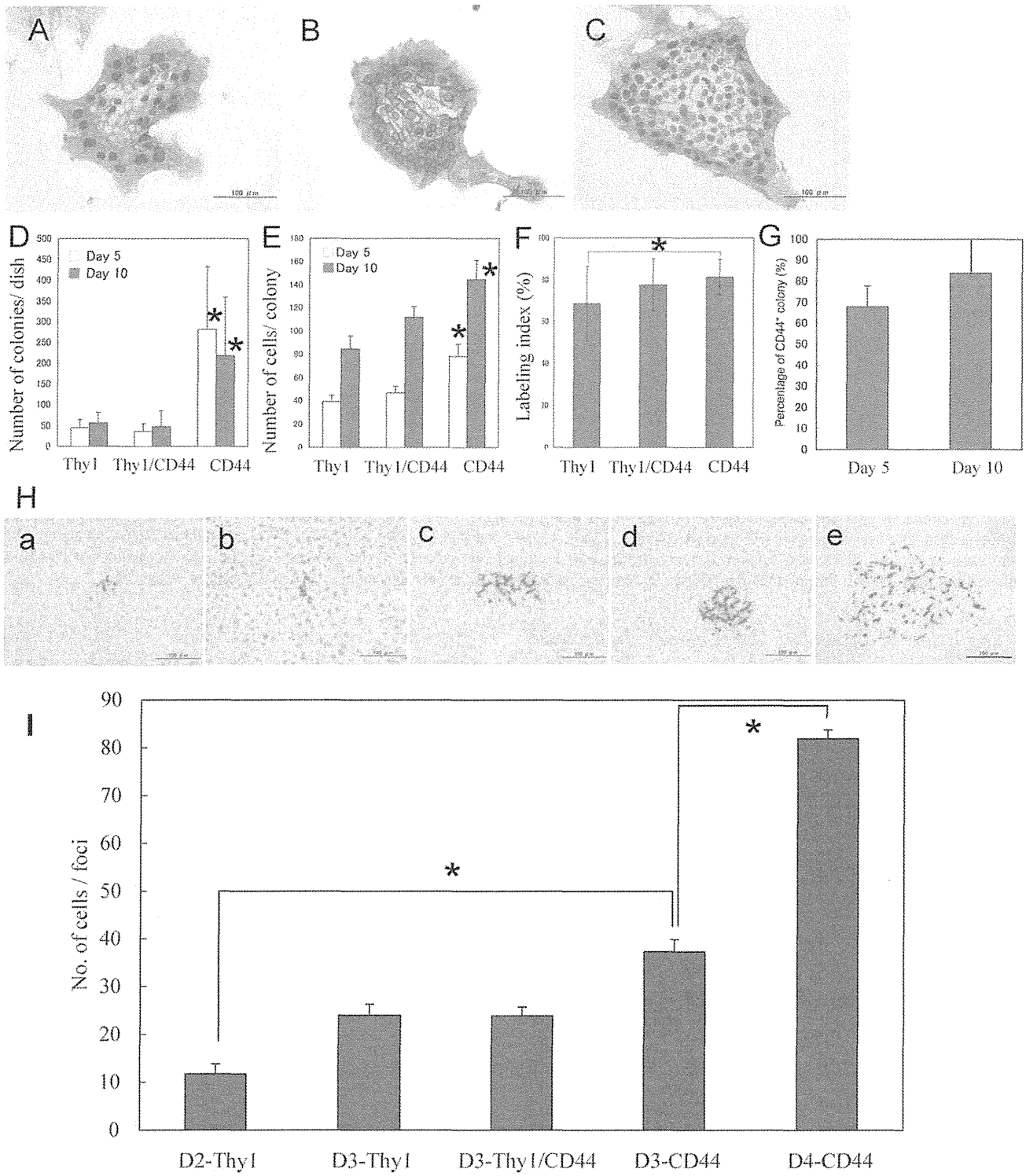

Fig. 4. Growth and CD44 positivity of epithelial cell colonies were examined in cultured cells. $Thy1^+$ (A), $Thy1^+/CD44^+$ (B), and $CD44^+$ cells (C) were isolated from GalN-D3 rat livers. Then, viable cells per dish (1×10^5) were plated on noncoated 35-mm culture dishes and cultured in the medium with EGF for 10 days. BrdU (40 μmol/L) was added to the medium 24 hours before fixation. At 5 and 10 days after plating, cells were fixed and double ICC for CD44 and BrdU was performed. CD44 and BrdU were stained violet and brown, respectively. Nuclei were counterstained with hematoxylin. The number of $CD44^+$ colony per dish (D), cells per colony (E), $BrdU^+$ cells per colony (F), and CD44 positivity of the colony derived from D2-$Thy1^+$ cells (G) were measured at 5 (white bar) and 10 days (gray bar) after plating. $CD44^+$ cell colonies were defined as colonies in which more than 90% of cells were stained with CD44. Asterisks show significant differences: $P < 0.05$. (D) $Thy1^+CD44^-$ and $Thy1^+CD44^+$ versus $Thy1^-CD44^+$ at days 5 and 10, (E) $Thy1^+CD44^-$ and $Thy1^+CD44^+$ versus $Thy1^-CD44^+$ at day 5, and $Thy1^+CD44^-$ versus $Thy1^-CD44^+$ at day 10, (F) $Thy1^+CD44^-$ versus $Thy1^-CD44^+$. Transplantation of isolated cells from GalN-treated livers into RET/PH-treated livers (H). Sorted GalN-D2-$Thy1^+$ (5×10^5 cells) (a), D3-$Thy1^+/CD44^-$ (b), D3-$Thy1^+/CD44^+$ (c), D3-$Thy1^-/CD44^+$ (d), or D4-$CD44^+$ cells (e) were intrasplenically transplanted into Ret/PH-treated rats. Thirty days after transplantation, livers were perfused with PBS, then sliced to make frozen sections. Tissues were enzymatically stained with DPPIV. DPPIV-positive cells are stained red. Nuclei are counterstained with hematoxylin (blue). The number of cells per focus was measured (I). Asterisks indicate significant differences: $P < 0.05$.

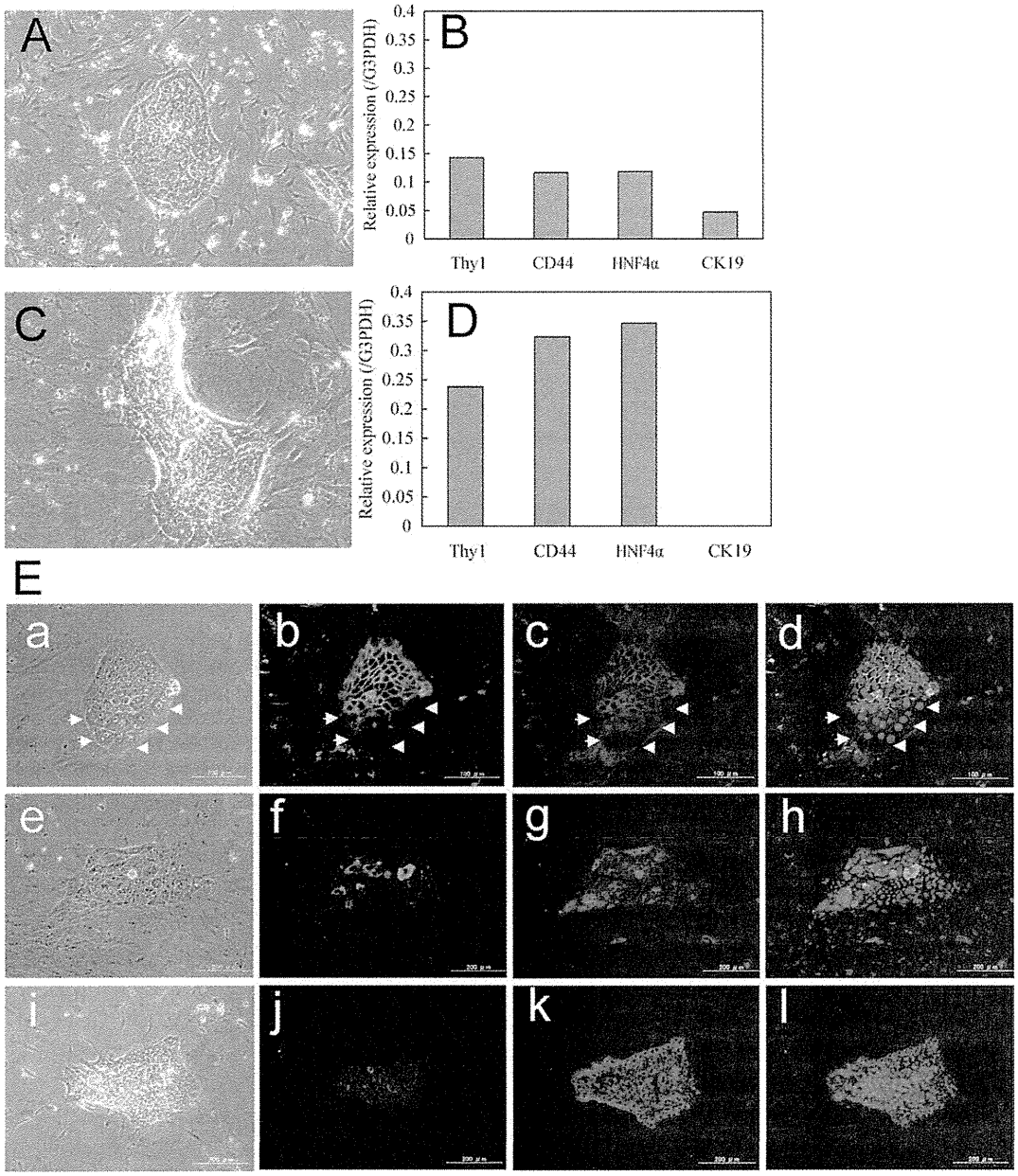

Fig. 5. Gene expression of the cells in each colony was measured by qPCR. Thy1^{+} cells sorted from GalN-D3 livers were cultured in the medium with EGF for 10 days. Each colony was separated from the dishes by using a cloning ring. Phase-contrast photos of all colonies were taken, then RNA of cells in the colonies was separated. qPCR was performed for each colony. Morphology (A and C) and gene expression (B and D) of representative colonies of CD44^{low} (A and B) and CD44^{high} (C and D) are shown. Cells were fixed at day 10, and double ICC for CD44/Thy1 (E, a-d) and CK-19/Alb (E, e-l) was performed. Although many cells in Thy1-derived colonies coexpressed CD44 and Thy1, some large cells (arrowheads) exhibited no expression of either protein (E, a-d). There were some colonies consisting of a mixture of Alb^{+} and CK-19^{+} cells (E, e-h), but most cells expressed Alb and only a few cells expressed CK-19 (E, i-l). Data for other colonies are shown in Supporting Fig. 2.

cloning ring. Phase-contrast photos were taken of every colony, and qPCR was performed. Gene-expression patterns of the colonies were roughly divided into two groups by the level of CD44 expression. Results for a representative colony in each group are shown in Fig. 5 (results for other colonies are shown in Supporting Fig. 2). Although intensity of gene expression varied among colonies, all colonies expressed CD44 messenger RNA (mRNA). Compared to cells in CD44^{low} colonies, those in CD44^{high} colonies showed not only relatively high expression of albumin and hepatocyte nuclear factor (HNF)-4α, but also suppression of CK-19 expression. Although coexpression of CD44 and Thy1 was observed in many Thy1-derived colonies, some large cells (arrowheads) exhibited no expression of either protein (Fig. 5E, a–d). There were colonies consisting of a mixture of albumin (Alb)$^{+}$ and CK-19^{+} cells (Fig. 5E, e–h), though most cells expressed

Alb and only a few cells exhibited CK-19 (Fig. 5E, i–l). To induce maturation of cells in Thy1-derived colonies, cells were treated with Matrigel. The treatment dramatically decreased Thy1 expression and increased levels of both HNF-4α and Alb (Supporting Fig. 3A). In addition, a marked increase of Alb secretion was also observed in cells with Matrigel (Supporting Fig. 3B). However, neither CD44 nor CK-19 expression was changed by the treatment.

Induction of Maturation in Cultured Cells. Next, we examined whether the newly generated hepatocytes could reconstruct hepatic organoids with highly differentiated functions. To enhance the organoid formation of colonies, colonies derived from D3-Thy1, CD44, and SHs from a healthy liver were replated on collagen-coated dishes to increase their density. In contrast to the Matrigel treatment, this procedure resulted in natural organoid formation, which consisted of piled-up cells with BCs. The expression of CCAAT/enhancer-binding protein (C/EBP)-α was ICC examined, and expression of genes related to hepatic differentiated functions was investigated by qPCR. In addition, to certify the function of the newly formed BCs, FD was added to the culture medium and the ability to secrete fluorescence into BCs was examined.

In spite of their origins, some cells in colonies became large and piled up with time after replating. Morphologically, BCs and cyst-like structures were observed in colonies, similar to those in colonies formed by SHs derived from healthy rat liver.[13,19,20] However, ICC for C/EBP-α revealed that the numbers of positive nuclei in Thy1- and CD44-derived colonies were smaller than in SH-derived colonies (Figs. 6A, B). Results of qPCR for each colony derived from Thy1, CD44, and SHs revealed that gene expression of cytochrome P450 1A2 (CYP1A2), tryptophan 2,3-dioxygenase (TDO), and carbamoylphosphate synthetase I (CPS-I), which are regarded as indicators for differentiated hepatic functions, was significantly higher in SH than CD44 or Thy1 (Fig. 6C). However, expression of tyrosine aminotransferase (TAT) was not different among cells.

In a SH-derived colony, fluorescence was secreted into BCs and accumulated in cysts (Fig. 7, e,f). The networks of BCs were well developed, corresponding to the regions of piled-up cells. On the other hand, in the colonies derived from both Thy1 (Fig. 7A, a,b) and CD44 cells (Figs. 7A, c,d), part of the region consisting of piled-up cells had a green, patch-like appearance. This phenomenon indicated the retention of fluorescence in the cytoplasm. In addition, to quantitatively compare structural differentiation among cells, the total length of BCs was measured in each colony. Total length of BCs was significantly larger in the SH-derived colony than in the Thy1- and CD44-derived colonies (Fig. 7B). These results suggested that newly generated hepatocytes derived from Thy1 and CD44 were not as mature as those from SHs.

Discussion

Hepatocytic Differentiation of Thy1-Positive Cells. Thy1 was first identified as a marker of oval cells by Petersen et al.[24] and then widely used in experiments with HPCs. Recently, a question was raised about the validity of Thy1 as a marker for oval cells.[25,26] It was reported that Thy1 was not a marker of oval cells, but of hepatic myofibroblasts and/or stellate cells. Although the issue regarding whether Thy1 is a marker for hepatic stem/progenitors is open to debate, we recently found that some $Thy1^+$ cells isolated from GalN-treated livers differentiated into $CD44^+$ hepatocytes through $Thy1^+CD44^+$ cells.[15] These results suggested that the population of $Thy1^+$ cells was heterogeneous, and that it contained putative hepatic stem cells possessing the ability to differentiate into hepatocytes. Interestingly, colony formation was clearly observed in the culture of cells from GalN-D3, whereas it was rarely observed in $Thy1^+$ cells isolated from GalN-D2, suggesting that $Thy1^+$ cells became the hepatic lineage between D2 and D3. In the present experiment, we demonstrated that EGF, fibroblast growth factor (FGF), and HGF might trigger the commitment to the hepatic lineage of $Thy1^+$ cells, some of which possess capability as putative stem cells. It has been reported that transforming growth factor (TGF)-α, HGF, and FGF play important roles in stem/progenitor cell-mediated liver regeneration. Indeed, the growth factors are transcriptionally upregulated during the period of active proliferation and differentiation of progenitor cells in rat liver[27–29] and appear to drive the early proliferation of the progenitor cell compartment.[27,30] Interestingly, it has been reported that stellate cells, which proliferate concomitantly and in close contact with progenitor cells,[31] appear to be the main source of TGF-α, HGF, and acidic FGF, whereas the corresponding cognate receptors are strongly expressed in progenitor cells, suggesting that the regulation of progenitor cell proliferation and differentiation by growth factors occurs primarily in a paracrine manner.[2,5] On the other hand, it is well known that priming factors are necessary for the emergence and proliferation of HPCs.[5,7] A correlation between the severity of liver disease and the magnitude

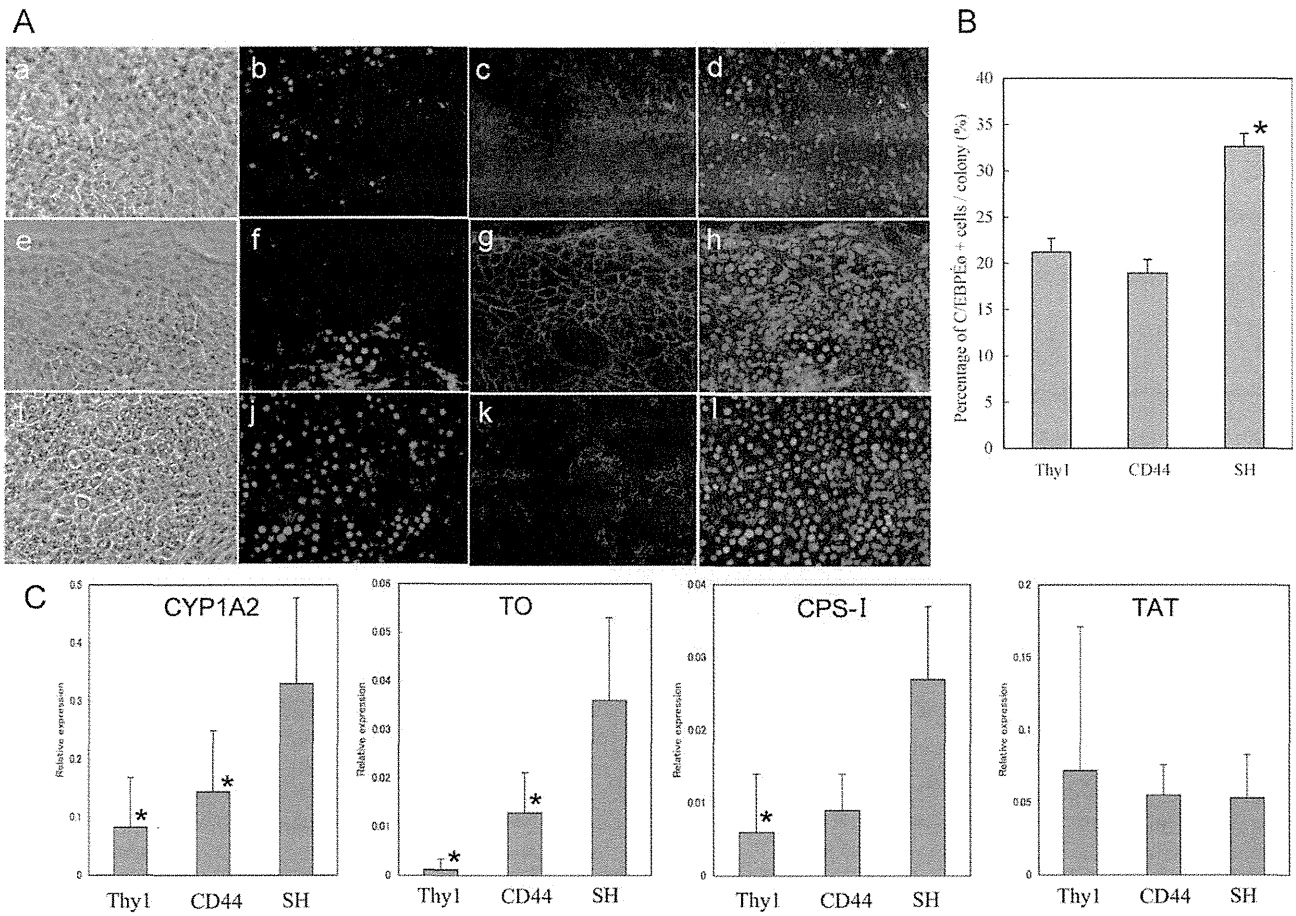

Fig. 6. To enhance organoid formation of the colonies, colonies derived from GalN-D3 Thy1 cells (A, a-d), CD44 cells (A, e-h), and a healthy liver (A, i-l) were replated on new collagen-coated dishes at 10 days after plating to increase the density of the colonies. Cells were cultured for more than 14 days after replating. This procedure resulted in natural organoid formation, which consisted of piled-up (matured) cells. The expression of C/EBP-α (A,b,f,j) and CD44 (A,c,g,k) was ICC observed and the percentage of C/EBP-α^+ cells per colony was measured (B). The gene expression of CYP1A2, TDO, CPS-I, and TAT in Thy1, CD44 cells, and SHs derived from a healthy liver was analyzed by real-time PCR (C). The scale is shown as a value relative to that of MH. Asterisks indicate a significant difference: $P < 0.05$, SH versus Thy1 or CD44.

of the response of hepatic progenitor cells has been reported and inflammatory cytokines, such as tumor necrosis factor alpha (TNF-α), interleukin (IL)-6, and interferon-gamma (INF-γ), were suggested to play central roles as priming factors in rodents.[32–36] However, in the present experiment, TNF-α, IL-6, and INF-γ could not induce the epithelial differentiation of Thy1$^+$ cells or enhance their expansion. This might be because D2-Thy1$^+$ cells have already been primed by the inflammation induced by GalN.

Expression of CD44 in Thy1-Derived Cells. In this experiment, we demonstrated that the growth and degree of hepatocytic differentiation of Thy1$^+$ cells were correlated with the expression of CD44. The results of GeneChip analysis demonstrated that the expression of genes related to hepatocytic differentiation, which were absent in GalN-D2-Thy1 cells, progressively increased in the order D3-Thy1, D3-Thy1$^+$CD44$^+$, and D4-CD44 cells. Although results of qPCR showed that the degree of expression of the genes of interest was different among epithelial colonies derived from D3-Thy1 cells, the cells in the CD44^{high} colonies showed high expression of Alb and HNF-4α, compared to cells in CD44^{low} colonies. In fact, CD44 expression in Thy1$^+$ cells increased with time in culture.

Acquisition of CD44 expression in Thy1$^+$ cells was also correlated with growth ability of cells. Growth of cells in CD44$^+$ cell-derived colonies was clearly faster than that of cells in colonies derived from Thy1-expressing cells. High growth activity of CD44$^+$ cells was also shown in the cell transplantation experiment. One month after transplantation, the number of cells in the foci derived from D4-CD44 was much larger than in those from Thy1-expressing cells. In general, the growth speed of cells shows an inverse correlation with degree of cell differentiation, and less-differentiated cells can proliferate much faster than differentiated cells. However, in the present experiment, although

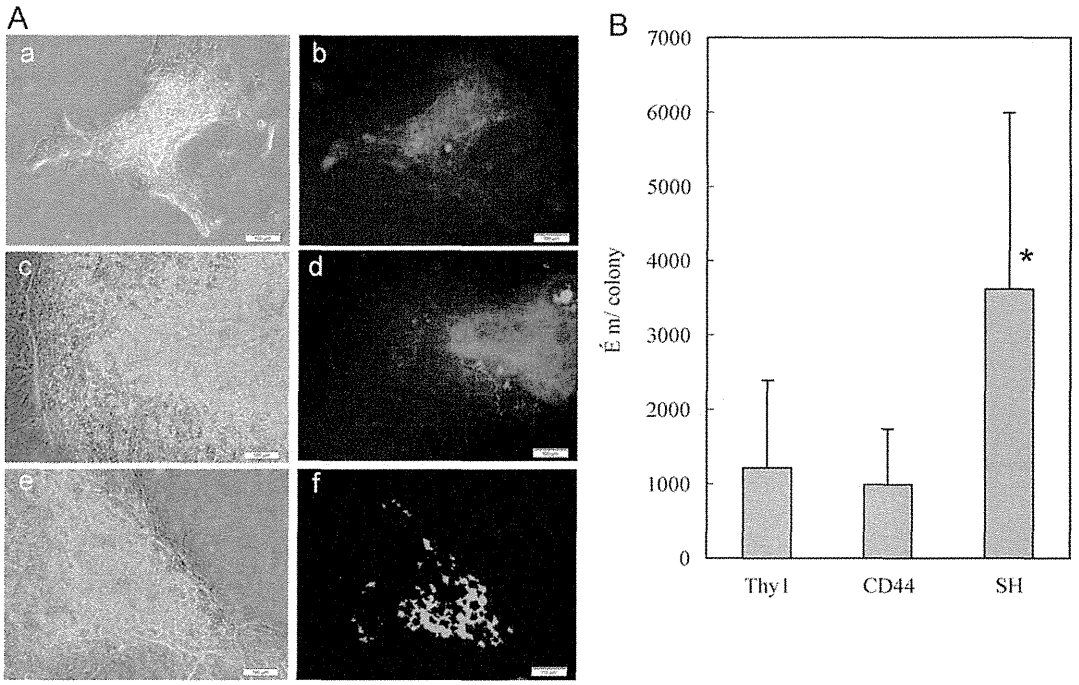

Fig. 7. To demonstrate the function of the newly formed BCs in hepatic organoids, FD was added to the culture medium and the ability to secrete fluorescence into BCs was examined. A part of the region consisting of piled-up cells in the colonies derived from both Thy1 (A, a,b) and CD44 cells (A, c,d) shows a green, patch-like appearance. Fluorescence was secreted into BCs and accumulated in the cysts in an SH-derived colony. To compare the development of BCs, the total length of BCs was measured in each colony (B). Total length of BCs was significantly larger in the SH-derived colony than in the Thy1- and CD44-derived colonies. Asterisk indicates a significant difference: $P < 0.05$, SH versus Thy1 and CD44.

$CD44^+$ cells were more differentiated than $Thy1^+$ cells, growth speed of $CD44^+$ cells was higher than that of CD44 cells (data not shown). At present, we cannot explain these findings, and further experiments will be required to clarify the regulatory mechanism of CD44 expression.

Restricted Maturation of HPCs. We previously reported that SHs derived from the healthy liver could spontaneously differentiate into hepatocytes that showed typical features of MHs and reconstructed three-dimensional (3D) structures by interacting with hepatic nonparenchymal cells.[11] In 3D structures, a complicated network of BCs is formed, and, when FD is added, fluorescence is secreted to BCs and expands all over the colony.[11,20] In the present experiment, despite their origins, cells could become large and pile up to form 3D structures that were morphologically similar to the hepatic organoids previously reported.[11,13] However, fluorescence was mostly retained in the cytoplasm of cells derived from both $Thy1^+$ and $CD44^+$ cells. Cytoplasmic retention of fluorescence indicates that cellular polarity is not well established, so that BCs cannot be well reconstructed. The short length of BCs also showed the incomplete maturation of both Thy1- and CD44-derived cells. Furthermore, compared to the organoids derived from SHs, CD44 expression remained and the ratio of C/EBP-α^+ cells was lower in organoids derived from both $Thy1^+$ and $CD44^+$ cells. The lower expression of CYP1A2, TDO, and CPS-I genes in organoids from Thy1 and CD44 than in those from SHs also indicated the immaturity of stem/progenitor cell-derived hepatocytes. These results demonstrated that the newly generated hepatocytes derived from $Thy1^+$ and $CD44^+$ cells might not have acquired the same highly differentiated functions as MHs. On the other hand, we previously reported that, compared to MHs, the repopulation efficiency of the liver by transplanted $Thy1^+$ cells was very low, and that most Thy1-derived foci disappeared within 2 months after transplantation.[16] Similar results were shown for the transplantation of $CD44^+$ cells. Those results indicate that HPCs may not be able to survive for a long time. Detailed histological analysis at 2 weeks after transplantation revealed that the percentage of C/EBP-α^+ cells in the early CD44-derived foci was lower than that in MH-derived foci. In addition, the size and shape of the cells and the distribution of the $DPPIV^+$ membrane were more irregular in Thy1- and CD44-derived foci than in MH-derived foci, which meant that BCs were not connected among cells, and that sinusoids were indistinct.[16] These cell-transplantation results may reflect the *in vitro* data shown in the present experiments. Shafritz et al.[6] summarized previous transplantation experiments using HPCs, and found that cells showed very low efficiency

of engraftment and repopulation, regardless of the condition of the recipient liver. Thus, hepatocytes induced from embryonic stem cells and other stem/progenitor cells have not yet matured to the stage at which they can efficiently repopulate the liver of an adult. In other words, to use HPCs in regenerative medicine, the state of differentiation of the cells used for cell transplantation may be very important, and a procedure for assessment of the maturation should be immediately developed.

Acknowledgments: The authors thank Ms. Minako Kuwano and Ms. Yumiko Tsukamoto for their technical assistance. The authors also thank Mr. Kim Barrymore for his help with the manuscript for this article.

References

1. Sell S. Heterogeneity and plasticity of hepatocyte lineage cells. HEPATOLOGY 2001;33:738-750.
2. Fausto N. Liver regeneration and repair: hepatocytes, progenitor cells, and stem cells. HEPATOLOGY 2004;39:1477-1487.
3. Michalopoulos GK. Liver regeneration: alternative epithelial pathways. Int J Biochem Cell Biol 2011;43:173-179.
4. Farber E. Similarities in the sequence of early histological changes induced in the liver of the rat by ethionine, 2-acetylaminofluorene, and 3'-methy-4-dimethylaminoazobenzene. Cancer Res 1956;16:142-149.
5. Santoni-Rugiu E, Jelnes P, Thorgeirsson SS, Bisgaard HC. Progenitor cells in liver regeneration: molecular responses controlling their activation and expansion. APMIS 2005;113:876-902.
6. Shafritz DA, Oertel M, Menthena A, Nierhoff D, Dabeva MD. Liver stem cells and prospects for liver reconstitution by transplanted cells. HEPATOLOGY 2006;43:S89-S98.
7. Bird TG, Lorenzini S, Forbes SJ. Activation of stem cells in hepatic diseases. Cell Tissue Res 2008;331:283-300.
8. Lemire JM, Shiojiri N, Fausto N. Oval cell proliferation and the origin of small hepatocytes in liver injury induced by D-galactosamine. Am J Pathol 1991;139:535-552.
9. Evarts RP, Hu Z, Omori N, Omori M, Marsden ER, Thorgeirsson SS. Precursor-product relationship between oval cells and hepatocytes: comparison between tritiated thymidine and bromodeoxyuridine as tracers. Carcinogenesis 1996;17:2143-2151.
10. Mitaka T, Kojima T, Mizuguchi T, Mochizuki Y. Growth and maturation of small hepatocytes isolated from adult liver. Biochem Biophys Res Commun 1995;214:310-317.
11. Mitaka T, Sato F, Mizuguchi T, Yokono T, Mochizuki Y. Reconstruction of hepatic organoid by rat small hepatocytes and hepatic nonparenchymal cells. HEPATOLOGY 1999;29:111-125.
12. Sasaki K, Kon J, Mizuguchi T, Chen Q, Ooe H, Oshima H, et al. Proliferation of hepatocyte progenitor cells isolated from adult human livers in serum-free medium. Cell Transplant 2008;17:1221-1230.
13. Sugimoto S, Mitaka T, Ikeda S, Harada K, Ikai I, Yamaoka Y, et al. Morphological changes induced by extracellular matrix are correlated with maturation of rat small hepatocytes. J Cell Biochem 2002;87:16-28.
14. Kon J, Ooe H, Oshima H, Kikkawa Y, Mitaka T. Expression of CD44 in rat hepatic progenitor cells. J Hepatol 2006;45:90-98.
15. Kon J, Ichinohe N, Ooe H Chen Q, Sasaki K, Mitaka T. Thy1-positive cells have bipotential ability to differentiate into hepatocytes and biliary epithelial cells in galactosamine-induced rat liver regeneration. Am J Pathol 2009;175:2362-2371.
16. Ichinohe N, Kon J, Sasaki K, Nakamura Y, Ooe H, Tanimizu N, et al. Growth ability and repopulation efficiency of transplanted hepatic stem, progenitor cells, and mature hepatocytes in retrorsine-treated rat livers. Cell Transplant 2012;21:11-22.
17. Gordon GJ, Coleman WB, Grisham JW. Temporal analysis of hepatocyte differentiation by small hepatocyte-like progenitor cells during liver regeneration in retrorsine-exposed rats. Am J Pathol 2000;157:771-786.
18. Chen Q, Kon J, Ooe H, Sasaki K, Mitaka T. Selective proliferation of rat hepatocyte progenitor cells in serum-free culture. Nat Protoc 2007;2:1197-1205.
19. Oshima H, Kon J, Ooe H, Hirata K, Mitaka T. Functional expression of organic anion transporters in hepatic organoids reconstructed by rat small hepatocytes. J Cell Biochem 2008;104:68-81.
20. Sudo R, Ikeda S, Sugimoto S, Harada K, Hirata K, Tanishita K, et al. Bile canalicular formation in hepatic organoid reconstructed by rat small hepatocytes and nonparenchymal cells. J Cell Physiol 2004;199:252-261.
21. Tanimizu N, Nishikawa M, Saito H, Tsujimura T, Miyajima A. Isolation of hepatoblasts based on the expression of Dlk/Pref-1. J Cell Sci 2003;116:1775-1786.
22. Goodison S, Urquidi V, Tarin D. CD44 cell adhesion molecules. Mol Pathol 1999;52:189-196.
23. Ponta H, Sherman L, Herrlich PA. CD44: from adhesion molecules to signalling regulators. Nat Rev Mol Cell Biol 2003;4:33-45.
24. Petersen BE, Goff JP, Greenberger JS, Michalopoulos GK. Hepatic oval cells express the hematopoietic stem cell marker Thy-1 in the rat. HEPATOLOGY 1998;27:433-445.
25. Dezsõ K, Jelnes P, László V, Baghy K, Bödör C, Paku S, et al. Thy-1 is expressed in hepatic myofibroblasts and not oval cells in stem cell-mediated liver regeneration. Am J Pathol 2007;171:1529-1537.
26. Dudas J, Mansuroglu T, Batusic D, Saile B, Ramadori G. Thy-1 is an *in vivo* and *in vitro* marker of liver myofibroblasts. Cell Tissue Res 2007;329:503-514.
27. Evarts RP, Hu Z, Fujio K, Marsden ER, Thorgeirsson SS. Activation of hepatic stem cell compartment in the rat: role of transforming growth factor α, hepatocyte growth factor, and acidic fibroblast growth factor in early proliferation. Cell Growth Differ 1993;4:555-561.
28. Marsden ER, Hu Z, Fujio K, Nakatsukasa H, Thorgeirsson SS, Evarts RP. Expression of acidic fibroblast growth factor in regenerating liver and during hepatic differentiation. Lab Invest 1992;67:427-433.
29. Hu Z, Evarts RP, Fujio K, Omori N, Omori M, Marsden ER, et al. Expression of transforming growth factor alpha/epidermal growth factor receptor, hepatocyte growth factor/c-*met*, and acidic fibroblast growth factor/fibroblast growth factor receptors during hepatocarcinogenesis. Carcinogenesis 1996;17:931-938.
30. Nagy P, Bisgaard HC, Santoni-Rugiu E, Thorgeirsson SS. *In vivo* infusion of growth factors enhances the mitogenic response of rat hepatic ductal (oval) cells after administration of 2-acetylaminofluorene. HEPATOLOGY 1996;23:71-79.
31. Paku S, Schnur J, Nagy P, Thorgeirsson SS. Origin and structural evolution of the early proliferating oval cells in rat liver. Am J Pathol 2001;158:1313-1323.
32. Nagy P, Kiss A, Schnur J, Thorgeirsson SS. Dexamethasone inhibits the proliferation of hepatocytes and oval cells but not bile duct cells in rat liver. HEPATOLOGY 1998;28:423-429.
33. Bisgaard HC, Müller S, Nagy P, Rasmussen LJ, Thorgeirsson SS. Modulation of the gene network connected to interferon-γ in liver regeneration from oval cells. Am J Pathol 1999;155:1075-1085.
34. Knight B, Yeoh GC, Husk KL, Ly T, Abraham LJ, Yu C, et al. Impaired preneoplastic changes and liver tumor formation in tumor necrosis factor receptor type 1 knockout mice. J Exp Med 2000;192:1809-1818.
35. Knight B, Matthews VB, Akhurst B, Croager EJ, Klinken E, Abraham LJ, et al. Liver inflammation and cytokine production, but not acute phase protein synthesis, accompany the adult liver progenitor (oval) cell response to chronic liver injury. Immunol Cell Biol 2005;83:364-374.
36. Matthews VB, Klinken E, Yeoh GC. Direct effects of interleukin-6 on liver progenitor oval cells in culture. Wound Repair Regen 2004;12:650-656.

Zoledronic Acid But Not Somatostatin Analogs Exerts Anti-Tumor Effects in a Model of Murine Prostatic Neuroendocrine Carcinoma of the Development of Castration-Resistant Prostate Cancer

Kohei Hashimoto,[1] Naoya Masumori,[1]* Toshiaki Tanaka,[1] Toshihiro Maeda,[1] Ko Kobayashi,[1] Hiroshi Kitamura,[1] Koichi Hirata,[2] and Taiji Tsukamoto[1]

[1]Department of Urology, Sapporo Medical University School of Medicine, Japan
[2]First Department of Surgery, Sapporo Medical University School of Medicine, Japan

BACKGROUND. Since neuroendocrine (NE) cells play an important role in the development of castration-resistant prostate cancer (CRPC), target therapy to NE cells should be considered for treating CRPC. We investigated the effects zoledronic acid (ZOL) and two somatostatin analogs (octreotide: SMS, and pasireotide: SOM) on an NE allograft (NE-10) and its cell line (NE-CS), which were established from the prostate of the LPB-Tag 12T-10 transgenic mouse.

METHODS. We examined the in vivo effects of ZOL, SMS and SOM as single agents and their combinations on subcutaneously inoculated NE-10 allografts and the in vitro effects on NE-CS cells. Apoptosis and cell cycle activity were assessed by immunohistochemistry using TdT-mediated dUTP-biotin nick-end labeling (TUNEL) and a Ki-67 antibody, respectively.

RESULTS. In vivo growth of NE-10 tumors treated with ZOL, ZOL plus SMS, or ZOL plus SOM was significantly inhibited compared to the control as a consequence of induction of apoptosis and cell cycle arrest. ZOL induced time- and dose-dependent inhibition of in vitro proliferation of NE-CS cells, but the somatostatin analogs (SMS and SOM) did not. ZOL also inhibited migration of NE-CS cells. These effects were caused by inhibition of Erk1/2 phosphorylation via impairment of prenylation of Ras.

CONCLUSIONS. ZOL, but not SMS or SOM, induced apoptosis and inhibition of proliferation and migration through impaired prenylation of Ras in NE carcinoma models. Our findings support the possibility that ZOL could be used in the early phase for controlling NE cells, which may trigger progression to CRPC. *Prostate 73: 500 511, 2013.*

KEY WORDS: **zoledronic acid; somatostatin analog; neuroendocrine carcinoma; prostate cancer; anti-tumor effect**

INTRODUCTION

Prostate cancer is the most common noncutaneus malignancy in men in developed countries [1]. Its incidence has been gradually increasing even in non-Caucasian men. As the growth of cancer cells is androgen-dependent, androgen deprivation therapy including surgical or chemical castration has been the mainstay of treatment for advanced prostate cancer. The response to this treatment lasts for a median of 36–48 months [2]. However, in most cases, the disease progresses despite the castration level of serum testosterone, and results in castration-resistant prostate cancer (CRPC). The prognosis of CRPC is poor and a concrete treatment strategy has not yet been established.

*Correspondence to: Naoya Masumori, Department of Urology, Sapporo Medical University School of Medicine S1, W16, Chuo ku, Sapporo 060 8543, Japan. E mail: masumori@sapmed.ac.jp
Received 4 June 2012; Accepted 27 August 2012
DOI 10.1002/pros.22590
Published online 19 September 2012 in Wiley Online Library (wileyonlinelibrary.com).

The exact mechanisms behind progression to castration resistance remain poorly understood. However, recent studies suggest that neuroendocrine (NE) cells, as well as pathways involving or bypassing the androgen receptor (AR), may play an important role in the development of castration resistance [3]. NE cells are present in both the normal and neoplastic prostate. They regulate surrounding prostate cells by secreting growth-modulating neuropeptides such as chromogranin A, serotonin and parathyroid hormone-related protein (PTHrP) [4]. Increases in the NE phenotype and secretory products are thought to be closely associated with progression and castration resistance in prostate cancer [5,6]. Previously, we developed an NE allograft (NE-10) and its cell line (NE-CS) from the prostate of the LPB-Tag 12T-10 transgenic mouse [7–9]. We demonstrated that secretions from NE cells induced androgen-independent growth of human prostate cancer cell line LNCaP and promoted pulmonary metastasis [10]. Therefore, it is crucial to seek a new drug or drug combinations targeting these prostatic NE carcinoma models (NE-10 and NE-CS).

Zoledronic acid (ZOL) is a nitrogen-containing bisphosphonate that inhibits bone resorption of osteoclasts through the inhibition of farnesyl-pyrophosphate synthetase in the mevalonate pathway. This agent has been demonstrated to have beneficial effects in patients with bone metastases of prostate cancer, reducing bone pain and skeletal-related events [11]. ZOL was also shown to have direct anti-tumor activity in several cancer cell lines. It is suggested that ZOL inhibits proliferation and induces apoptosis by impairment of prenylation of Ras and other small GTP-binding proteins (G proteins) [12].

Somatostatin is a peptide hormone that regulates secretion of various exocrine and endocrine glands via specific somatostatin receptors (SSTR). Five different subtypes (SSTR1-5), which are coupled to G proteins, have been identified [13]. Since a majority of NE tumors predominantly express SSTR2, somatostatin analogs having high affinity for SSTR2a such as octreotide (SMS) are considered to be drugs for NE tumors [14,15]. Since several studies have reported that SSTR1 and SSTR5 are expressed in addition to SSTR2 in prostate cancer tissue [15,16], new somatostatin analogs such as pasireotide (SOM) that have high affinity for SSTR5 in addition to SSTR2 [17], may be useful as new drugs for prostatic NE carcinoma.

In the present study, we investigated whether the growth of NE carcinoma models (NE-10, NE-CS) could be influenced by ZOL and/or somatostatin analogs (SMS and SOM), having potential anti-tumor activities.

MATERIALS AND METHODS

Cell Lines and Lell Culture

NE-CS is a murine prostate neuroendocrine cancer cell line established in our institute [9]. It was derived from an NE-10 tumor [8]. Passage numbers between 12, and 16 were used in the study. The NE-CS cells were maintained in the culture medium described below in 5% CO_2 in a humidified incubator. The medium consisted of RPMI-1640 (Gibco BRL, Breda, The Netherlands) that was supplemented with MEM nonessential amino acid (10 ml/L, Gibco BRL), MEM sodium pyruvate, penicillin–streptomycin (10 ml/L, Gibco BRL), 10% fetal bovine serum (FBS, ICN Biomedicals, Costa Mesa, CA), and 7.5% $NaHCO_3$.

ReverseTranscription Polymerase Chain Reaction (RT-PCR) Analysis

To investigate expression of SSTR in NE-10, RT-PCR analysis was performed. Tumor tissues in allografts of NE-10 were homogenized. Total RNA was extracted using an RNeasy kit (Qiagen, Valencia, CA) according to the manufacturer's instructions. A total of 2 μg of total RNA was reverse transcribed in a thermal cycles (Perkin–Elmer, Norwalk, CT) using SuperScript III (Invitrogen, Carlsbad, CA) and oligo (dT) 12–18 primers according to the manufacturer's instructions for 1 hr at 50°C in a 40 μl reaction mixture. Resulting cDNA (1 μl) was amplified with Taq polymerize and one set of oligonucleotide primers. Samples were denatured for 5 min at 94°C, and then amplified for 35 cycles at 94°C for 30 sec, 57°C for 30 sec, and 72°C for 1 min. Aliquots (9 μl) from each PCR sample were then analyzed by agarose-gel electrophoresis. Forward and reverse primer sequences were as follows: SSTR2a (5′-CAGCTGTACCATCAACTGGC, 5′-ATTTGTCCTGCTTACTGTCG), SSTR2b (5′-TGATCAATGTAGCTGTGTGG, 5′-CAAAGAACATTCTGGAAGC), SSTR5 (5′-TGCCTGATGGTCATGAGTGT, 5′-GGAAACTCTGGCGGAAGTTA), GAPDH (5′-TACAGCAACAGGGTGGTGGA, 5′-ACCACAGTCCATGCCATCAC).

Growth of NE-10 Allografts In Vivo

To examine the in vivo effects of ZOL, SMS and SOM as single agents and their combinatorial effects on prostatic NE carcinoma, we used NE-10 allografts. Six-week-old male BALB/c nude mice were castrated using the scrotal approach. After one week, 50 mg tissue fragments of the NE-10 allograft were inoculated subcutaneously (s.c.) into the flanks of mice. Two weeks after transplantation, NE-10 tumors grew to a volume of more than 100 mm^3. The mice were then